

## **Design and Synthesis of N-3-Substituted Quinazolinone Derivatives as Anticancer Agents Targeting EGFR**

Pritam Maity<sup>a</sup>, Poonam Yadav<sup>b</sup>, Joydeep Chatterjee<sup>a</sup>, Madhurendra Kumar Katiyar<sup>a</sup>, Umashanker Navik<sup>b#</sup>, Raj Kumar<sup>a\*</sup>

*<sup>a</sup>Laboratory for Drug Design and Synthesis, Department of Pharmaceutical Sciences and Natural Products, School of Health Sciences, Central University of Punjab, Bathinda 151401, India*

*<sup>b</sup>Department of Pharmacology, School of Health Sciences, Central University of Punjab, Bathinda 151401, India*

\*Correspondence: Email: [raj.khunger@gmail.com](mailto:raj.khunger@gmail.com); [raj.khunger@cup.edu.in](mailto:raj.khunger@cup.edu.in) (RK; ORCID ID: [orcid.org/0000-0001-5113-6627](https://orcid.org/0000-0001-5113-6627))

# Co-correspondence: Email: [uma.shanker@cup.edu.in](mailto:uma.shanker@cup.edu.in)

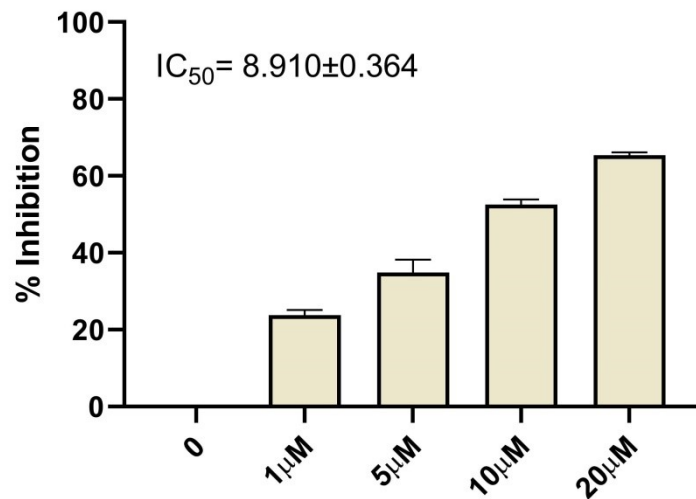


Fig. S1 Antiproliferative activities of 4c at 1, 5, 10, and 20 μM conc. for 24h against PC-3 cells. Data are presented as mean ± SEM for three independent experiments.

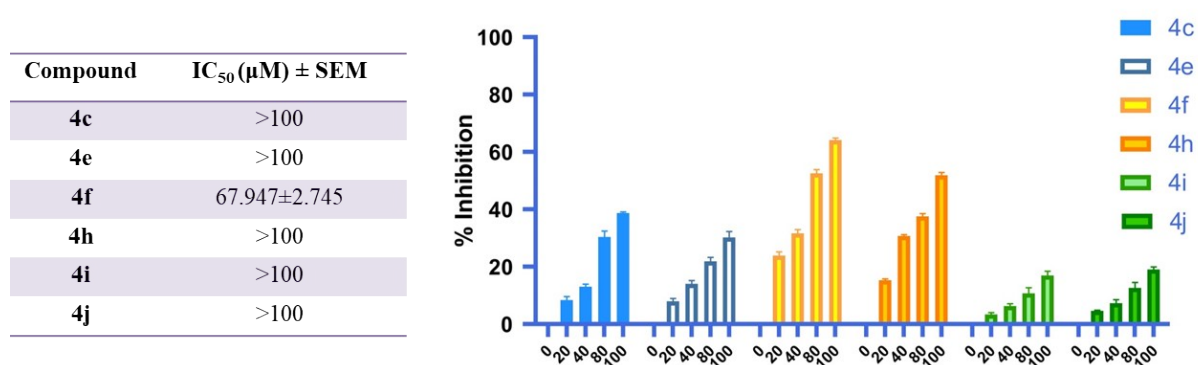
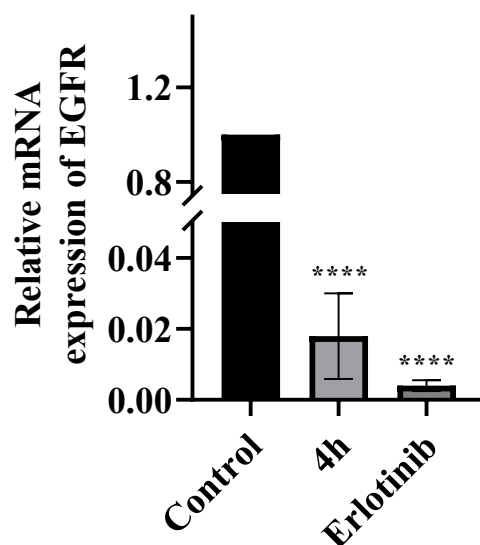


Fig. S2 Antiproliferative activities of 4c, 4e, 4f, 4h, 4i and 4j against HEK-293 cells at 20, 40, 80 and 100 μM concentration. Data are presented as mean ± SEM for three independent experiments.



**Fig. S3** Effect of 4h on relative mRNA expression of EGFR in MCF-7 cell line. All values are expressed as mean  $\pm$  SEM. Analysis was done using one-way ANOVA followed by Tukey's Post hoc test. \*\*\*\* $p < 0.0001$  "\*" versus control.

**Table S1:** Selectivity Index of compound 4c, 4e, 4f, 4h, 4i and 4j against MCF-7 compared

MCF-7	
Compound	Selective index
4c	>17
4e	>15
4f	10.49
4h	>15
4i	>13
4j	>16

#### MM-GBSA study:

##### Results:

The binding free energies of the 4h and 4i were calculated using the MM-GBSA (molecular mechanics generalized born surface area). The binding energy ( $\Delta G$  Bind), the Coulomb energy contribution ( $\Delta G$  Coulomb), the van der Waals energy contribution ( $\Delta G$  van der Waals) and the lipophilic energy contribution ( $\Delta G$  Lipo) are tabulated in Table 2. Compound 4i showed an improved  $\Delta G$  Bind,  $\Delta G$  Coulomb,  $\Delta G$  vdW, and  $\Delta G$  Lipo energy compared to 4h.

Table S2: MM-GBSA binding free energy results of compounds 4h and 4i against EGFR

Entry	$\Delta G$ Bind	$\Delta G$ Bind Coulomb	$\Delta G$ Bind vdW	$\Delta G$ Bind Lipo
4i	-46.22	-11.21	-44.65	-13.51
4h	-39.76	-7.86	-41.47	-12.21

##### Methods:

The binding energy of the ligand in the EGFR binding pocket was analyzed by molecular mechanics with generalized Born and surface area solvation (MM-GBSA) study. The docking output file was incorporated into the MMGBSA study in the 'Prime' module of Maestro. The docking complexes were minimized, and binding energies were calculated using the VSGB solvation model.



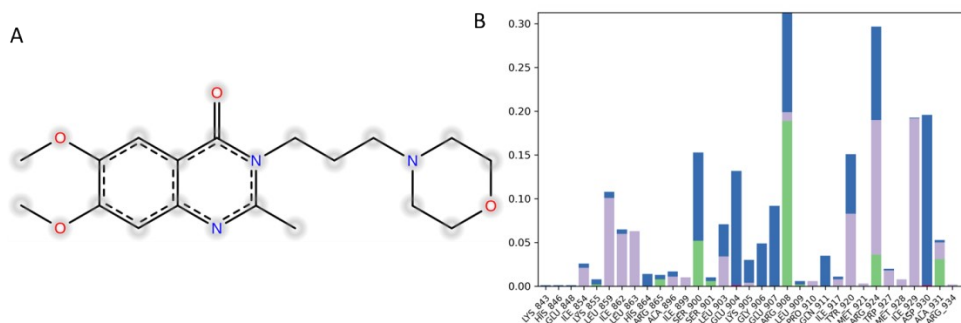


**Fig. S6** 2D Protein-ligand interaction diagram (A) and Protein-ligand interaction histogram (B) from the MD simulations of **4i** in the EGFR binding site; (H-bonds are shown in green, and lipophilic contacts in grey).

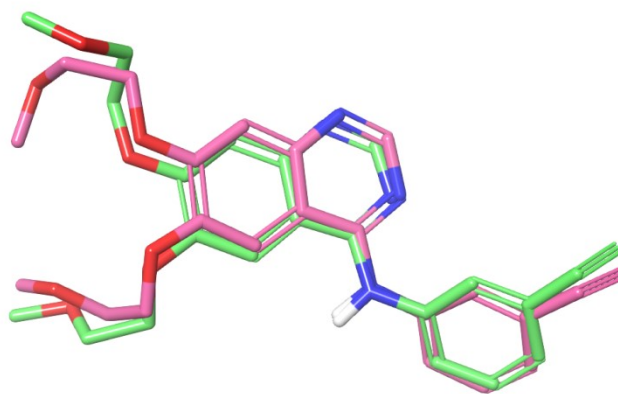
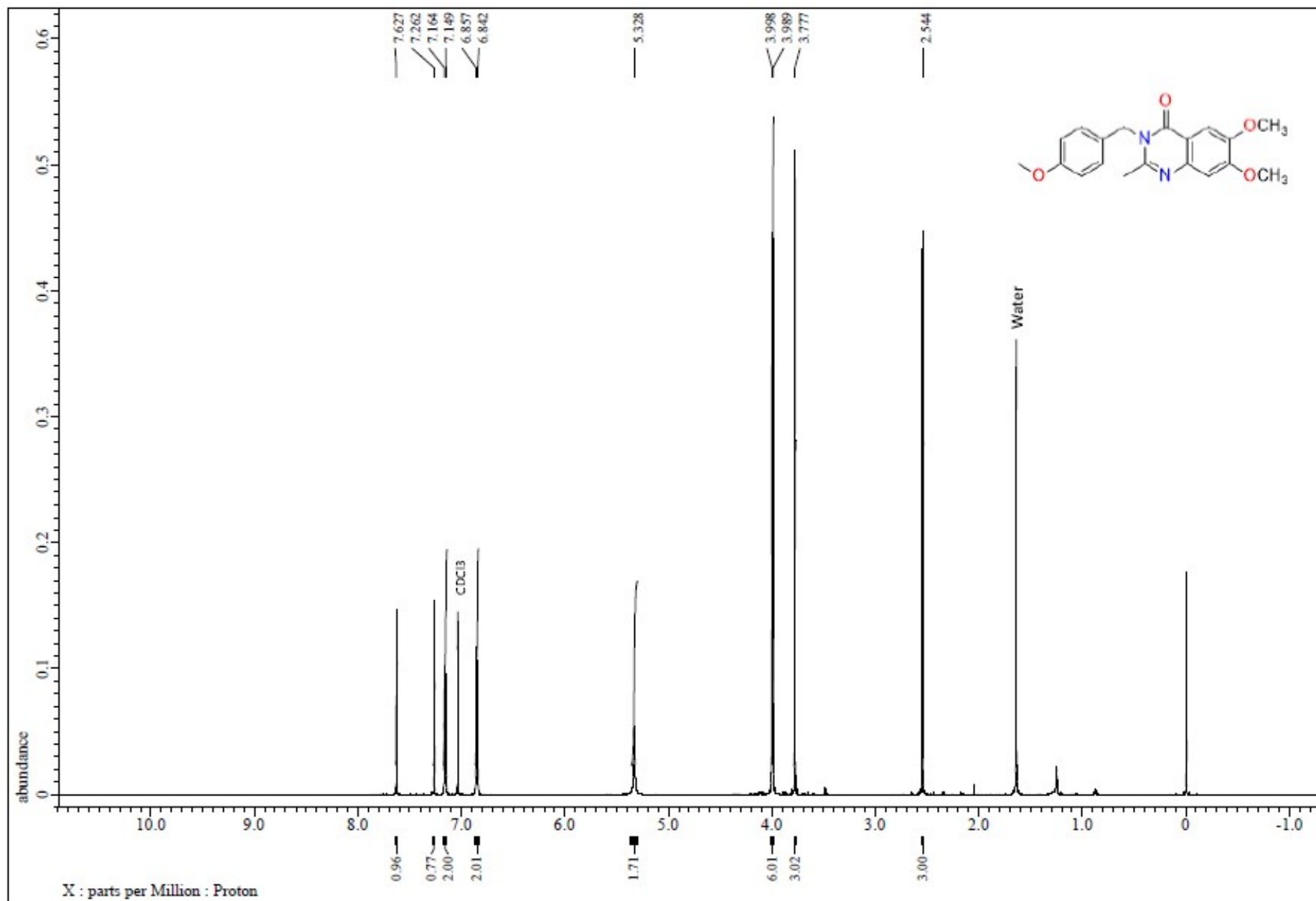


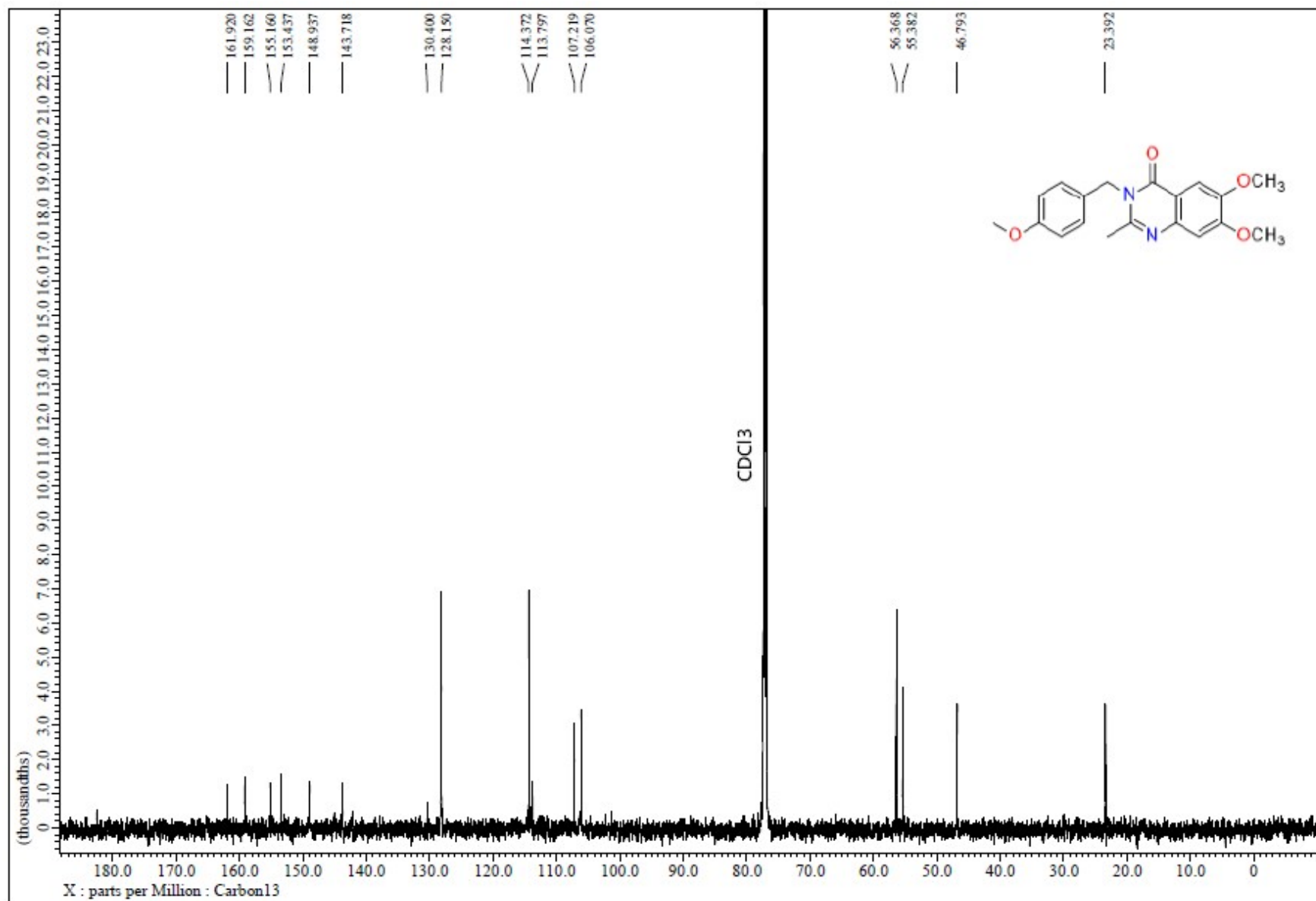
**Fig. S7** Superimposed structures (with RMSD 1.01Å) of co-crystallized erlotinib (green) and re-docked erlotinib (pink) at the binding pocket of EGFR.

$^1\text{H}$ ,  $^{13}\text{C}$  NMR and HRMS of all synthesized final compounds (4a-4j)

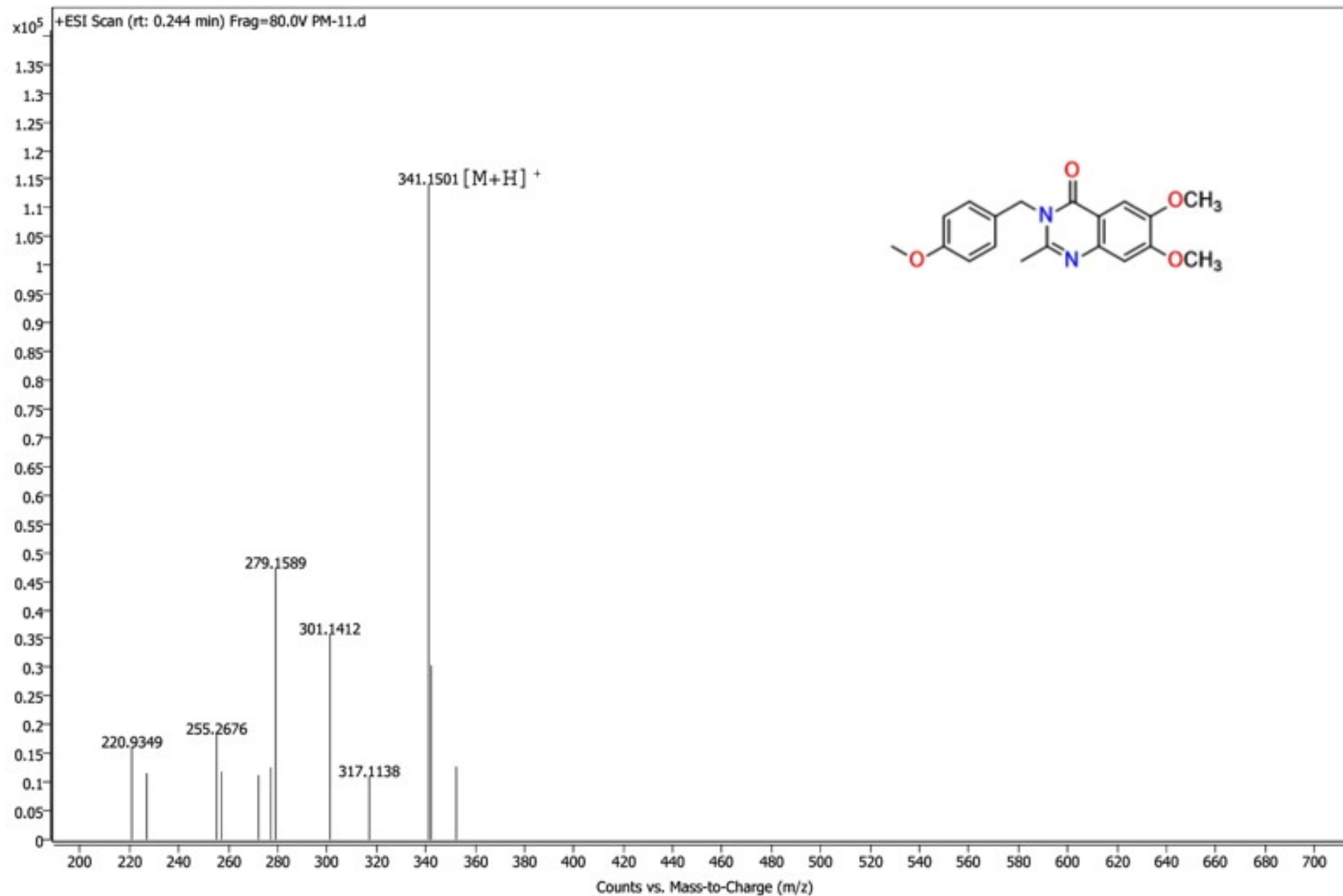
$^1\text{H}$  NMR of **4a**



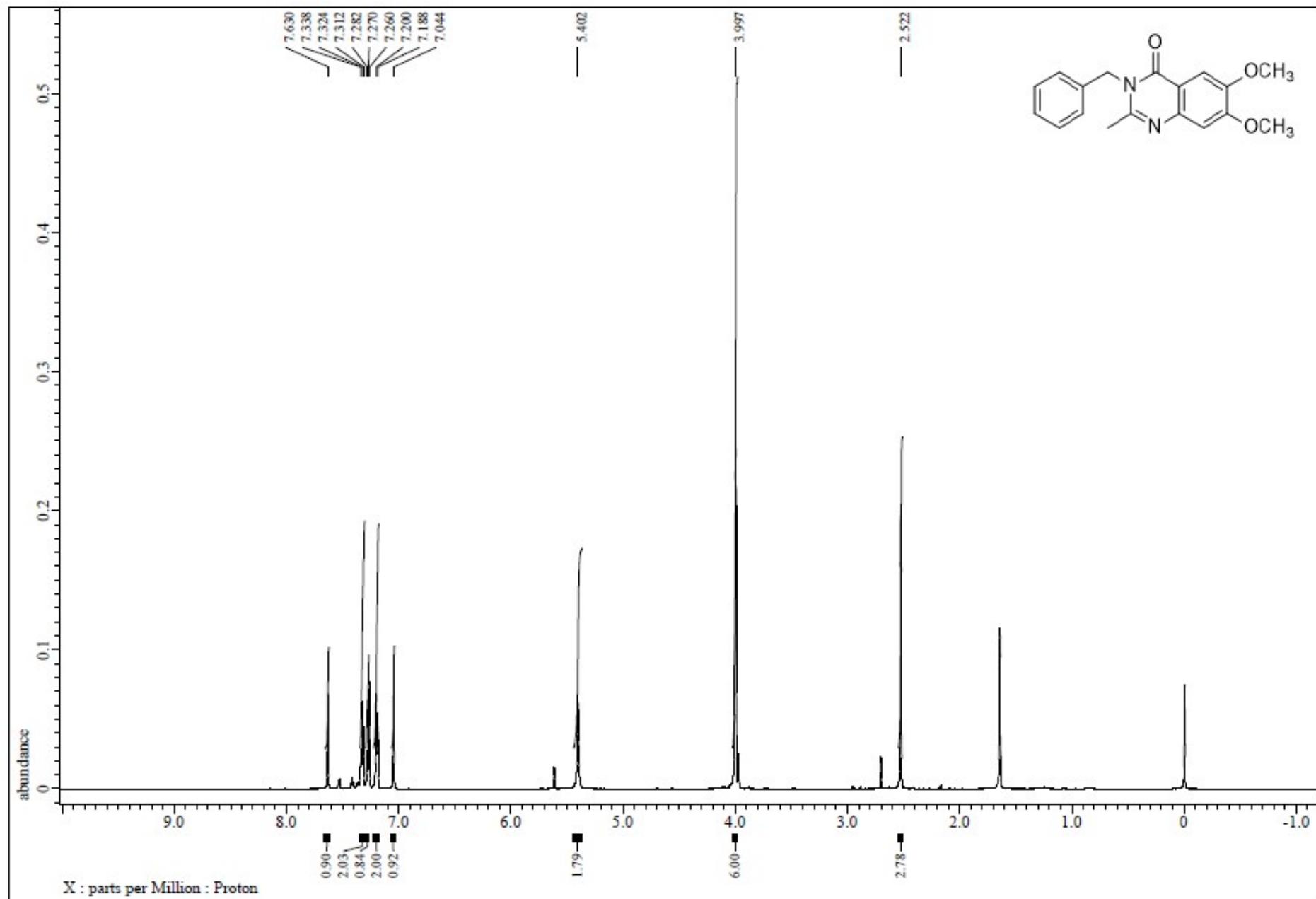
<sup>13</sup>C NMR of 4a



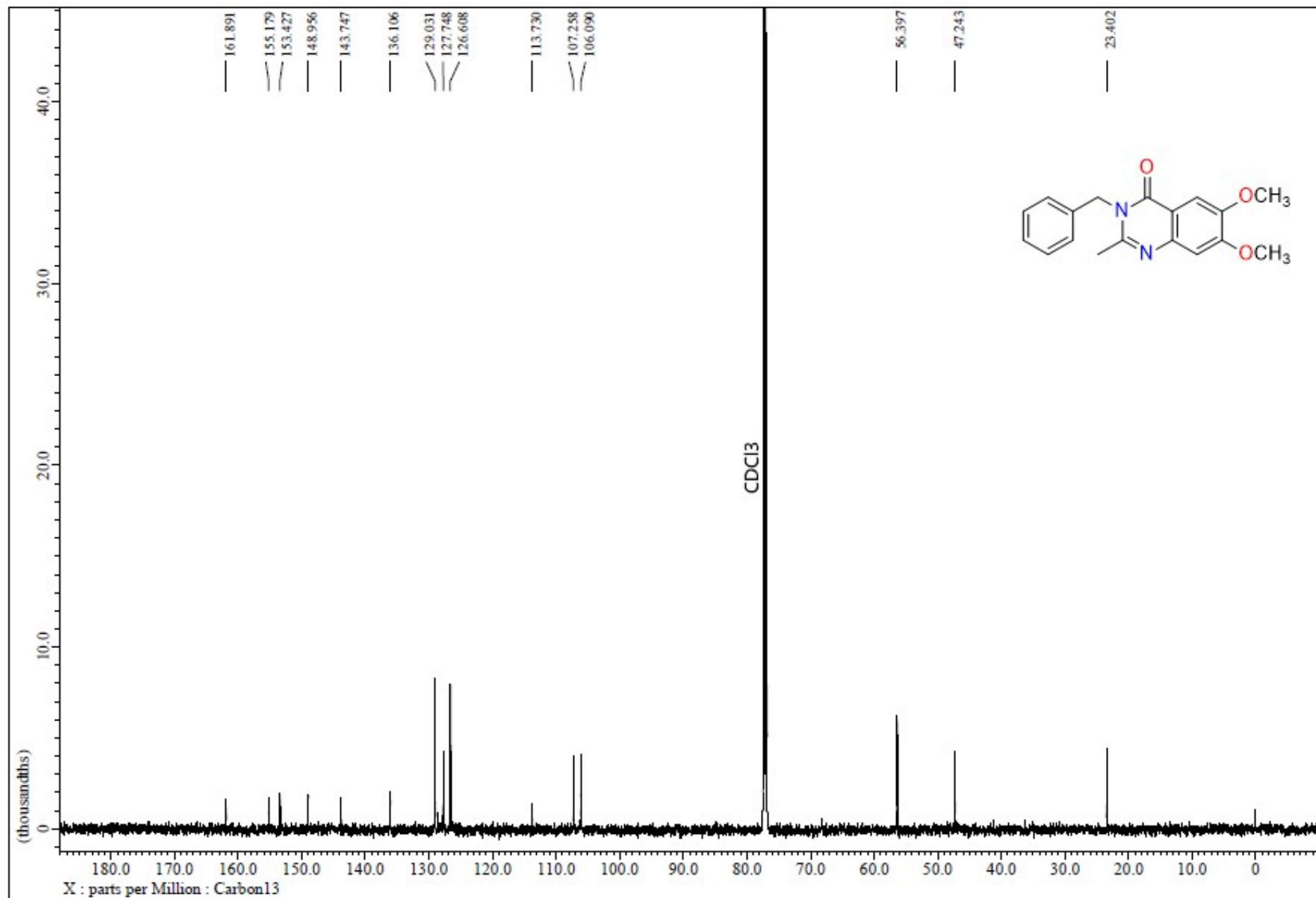
## HRMS of 4a



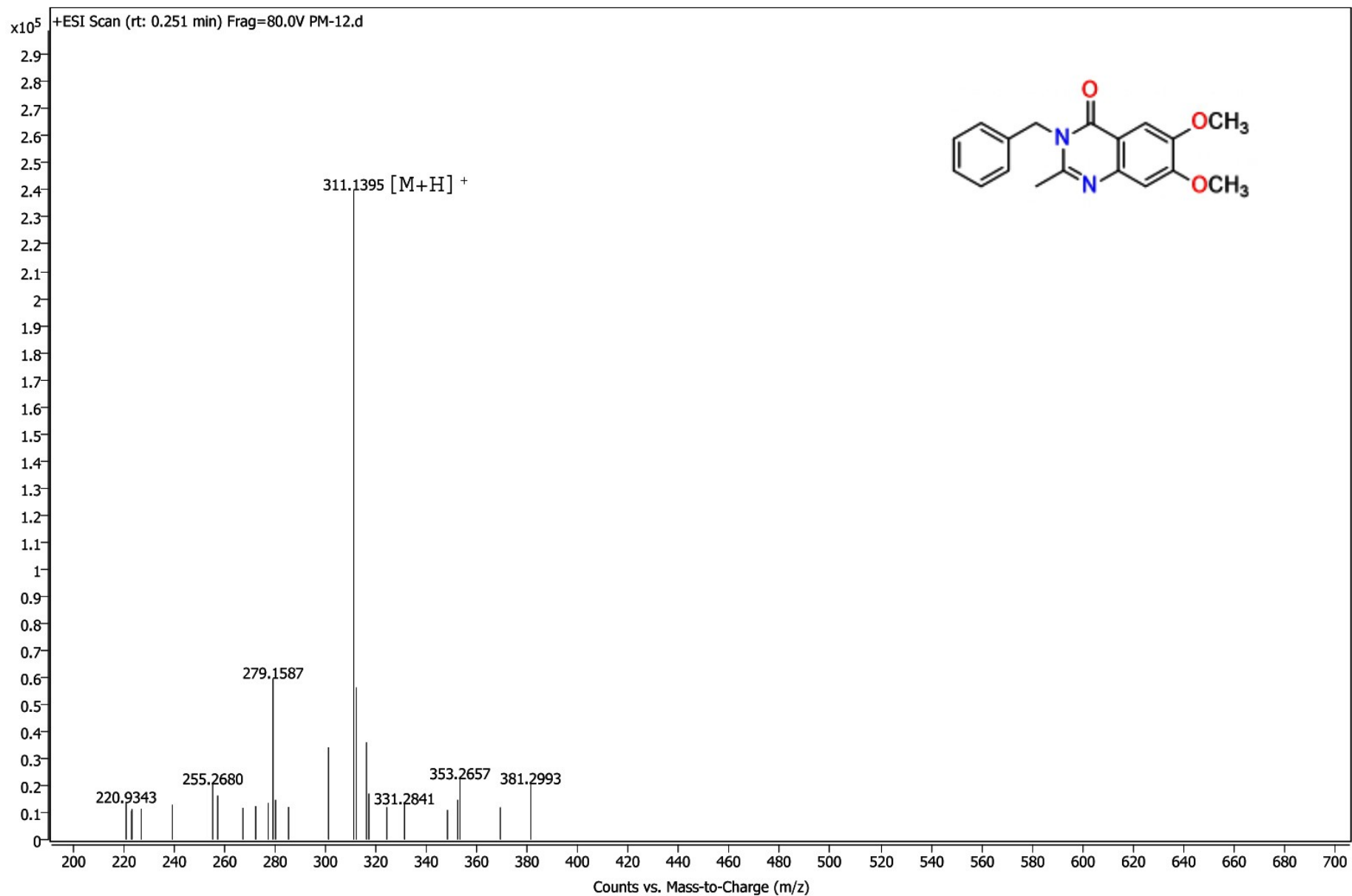
$^1\text{H}$  NMR of **4b**



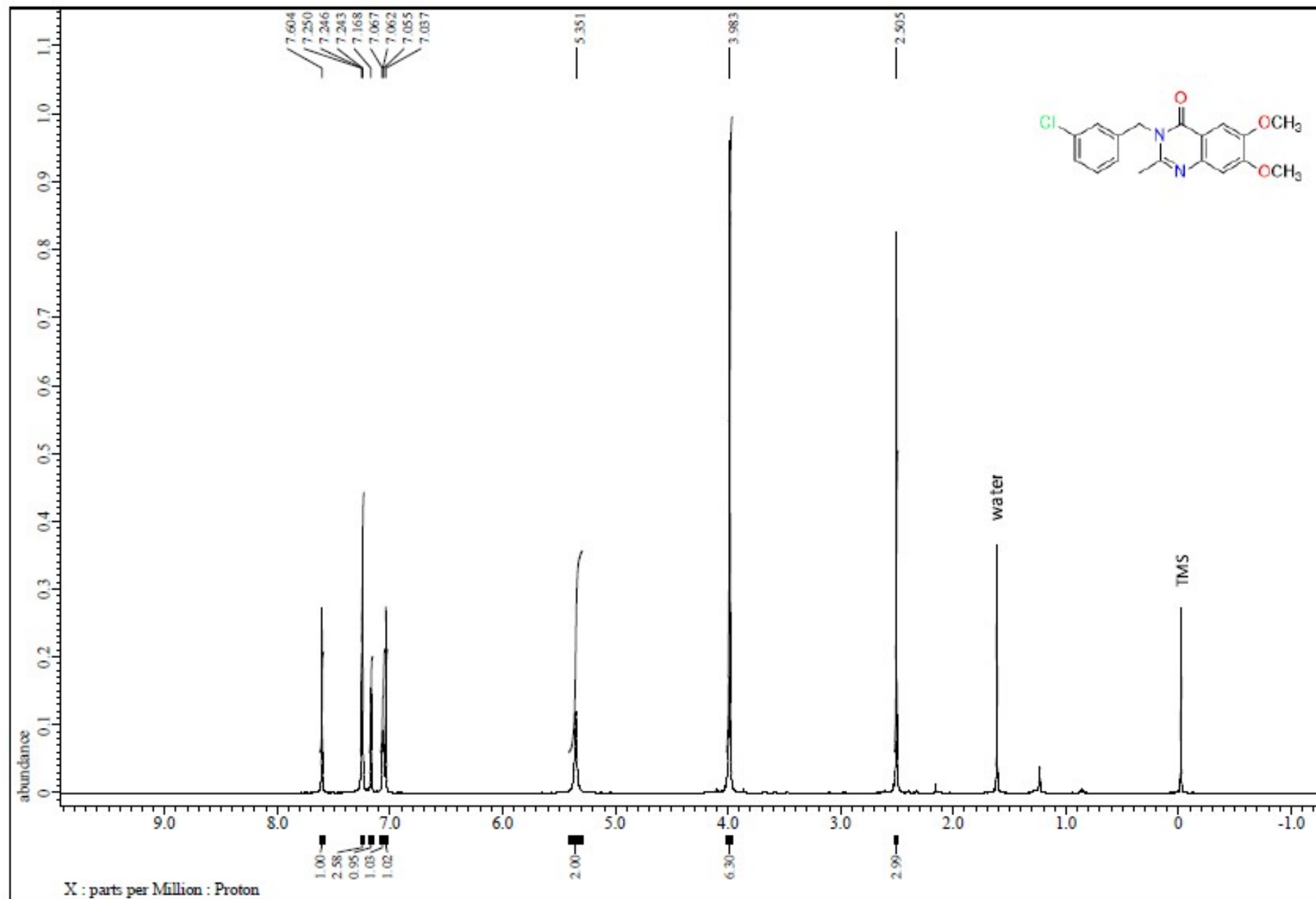
<sup>13</sup>C NMR of **4b**



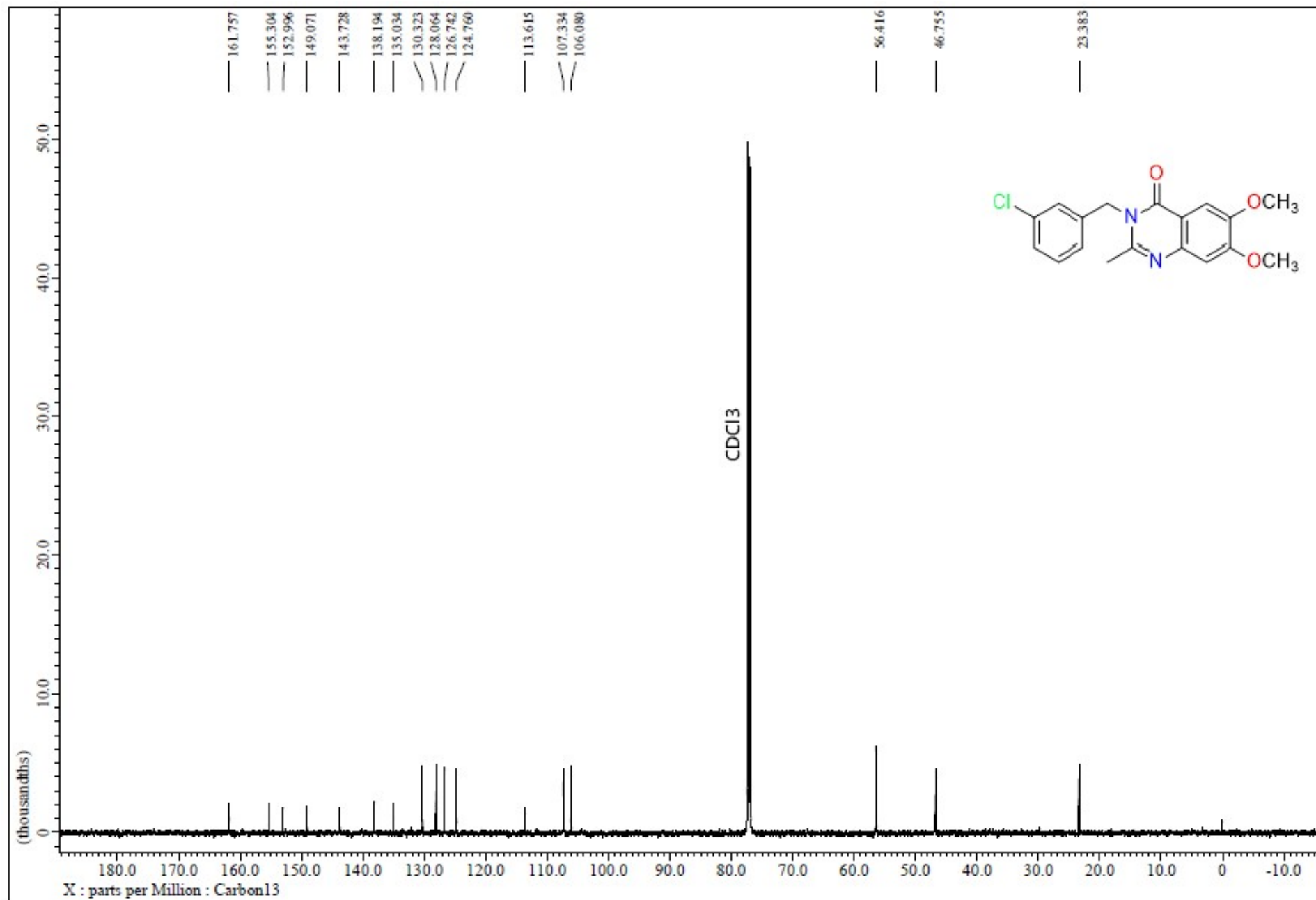
# HRMS of 4b



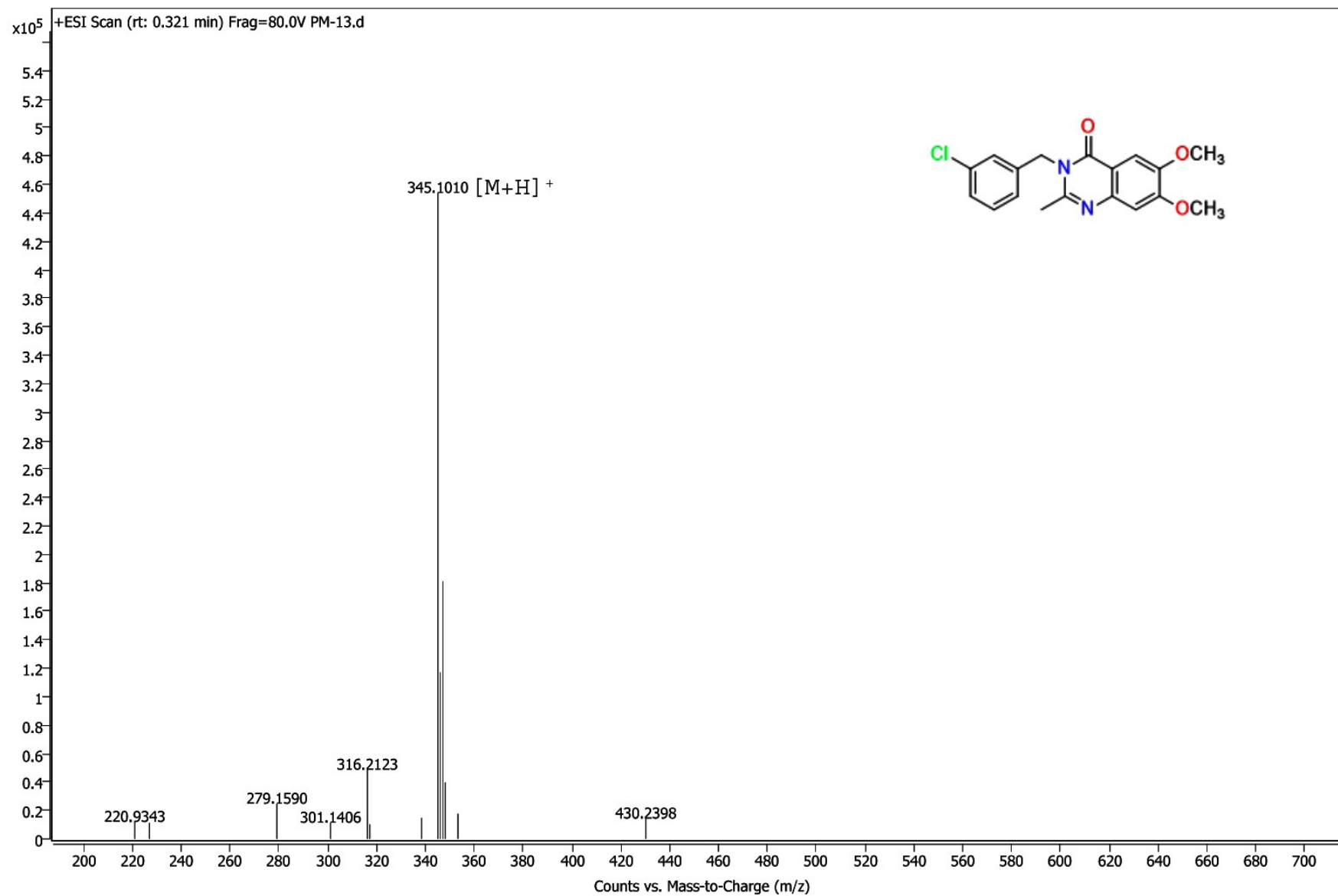
$^1\text{H}$  NMR of **4c**



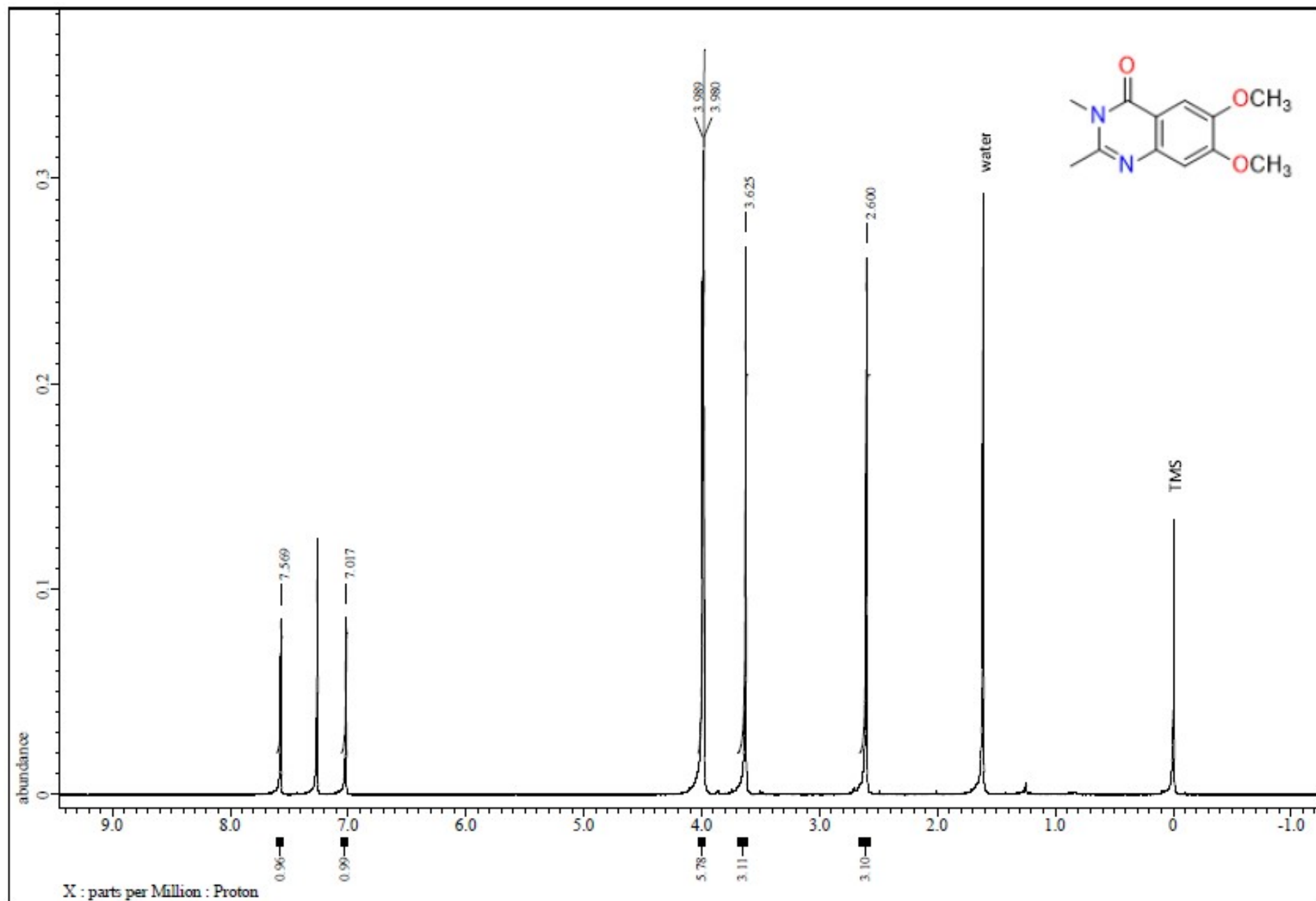
<sup>13</sup>C NMR of 4c



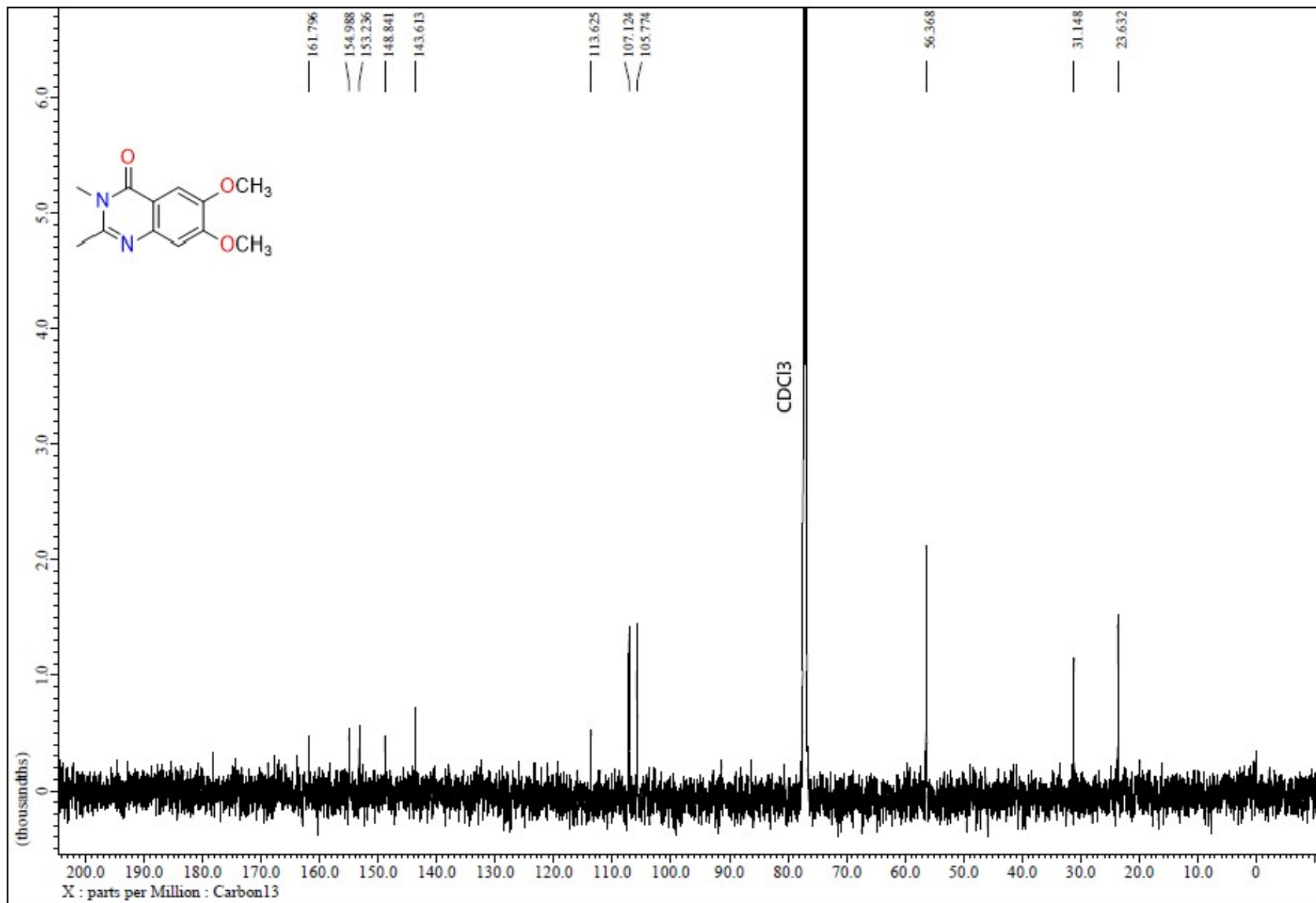
# HRMS of 4c



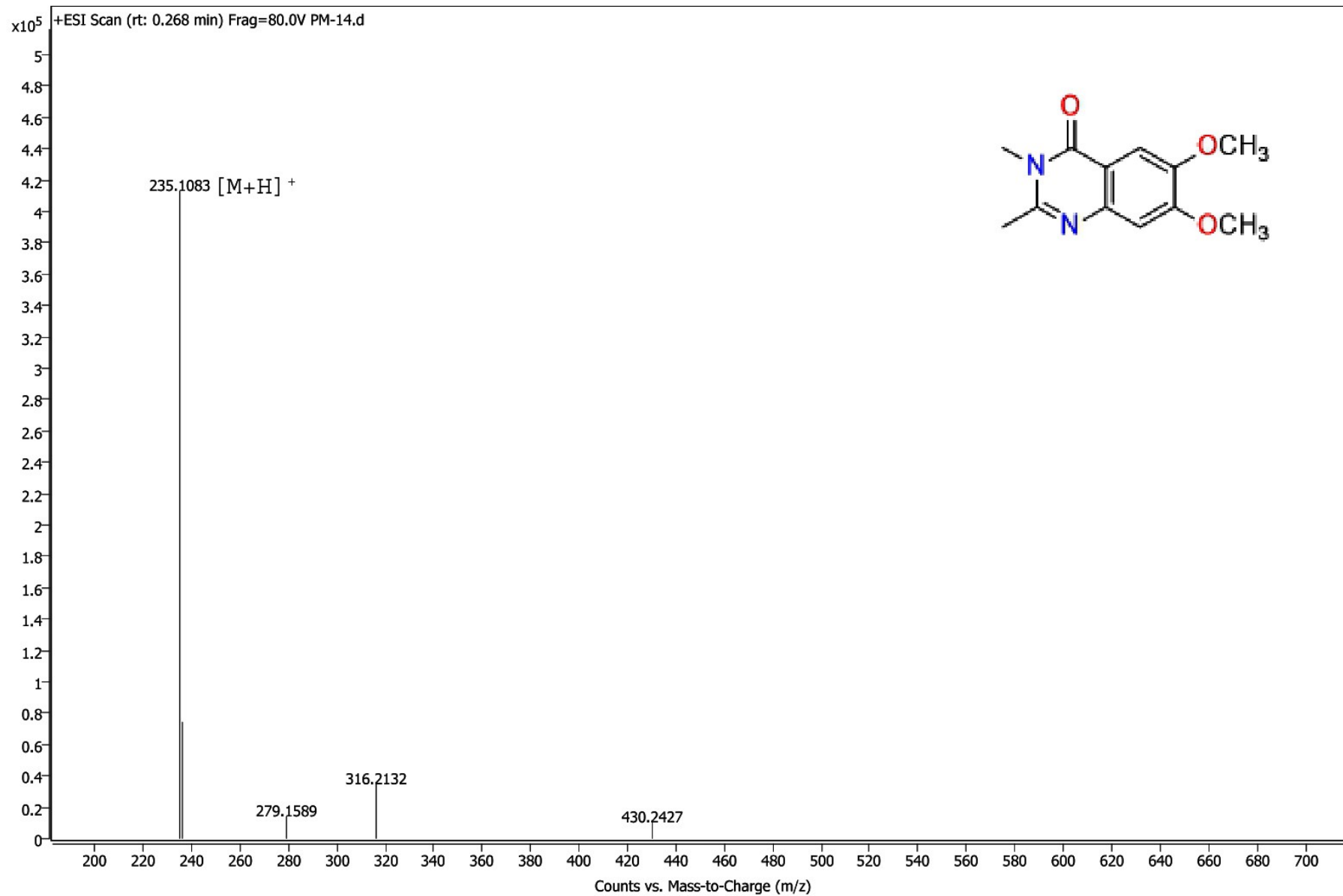
$^1\text{H}$  NMR of **4d**



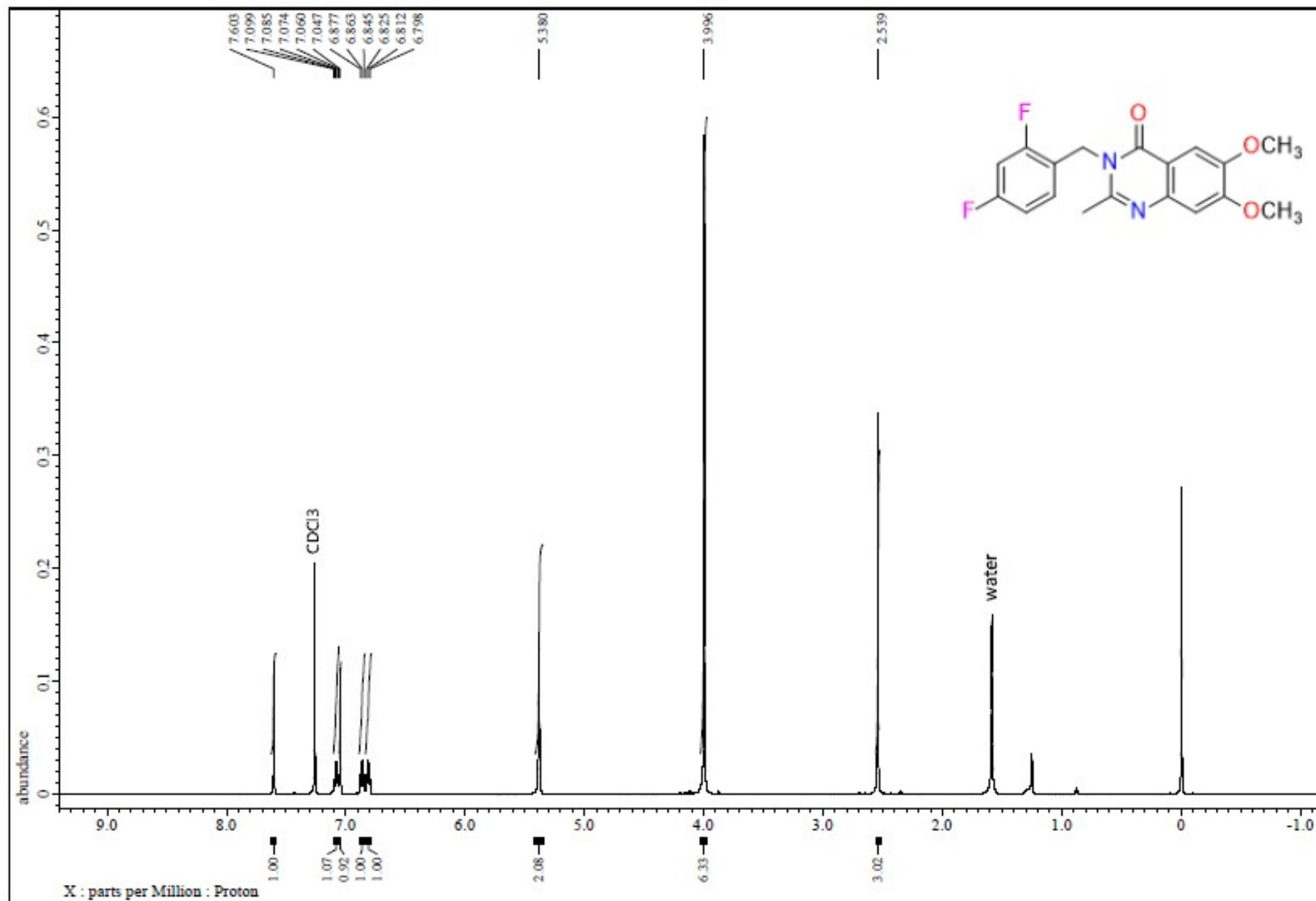
<sup>13</sup>C NMR of **4d**



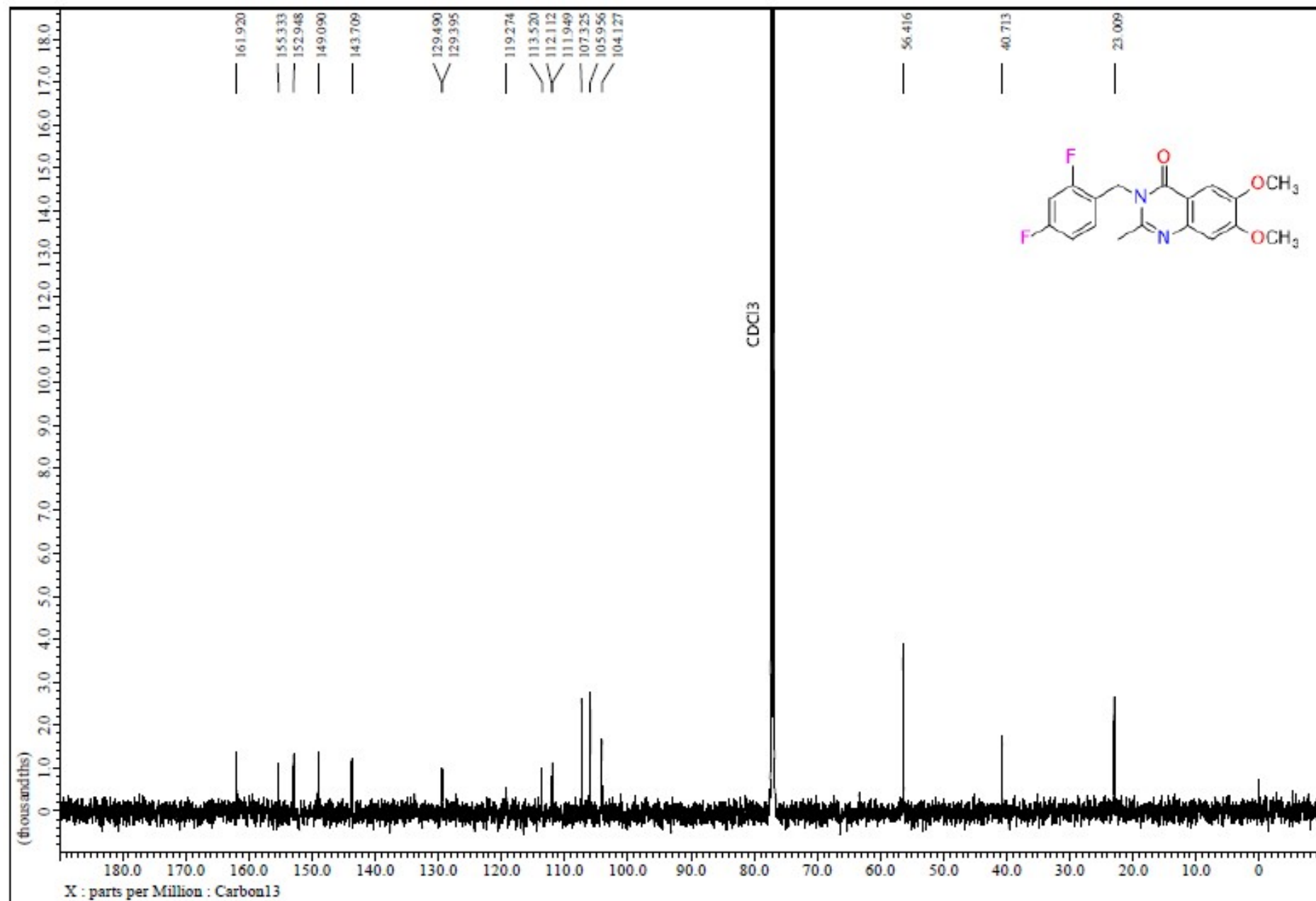
# HRMS of 4d



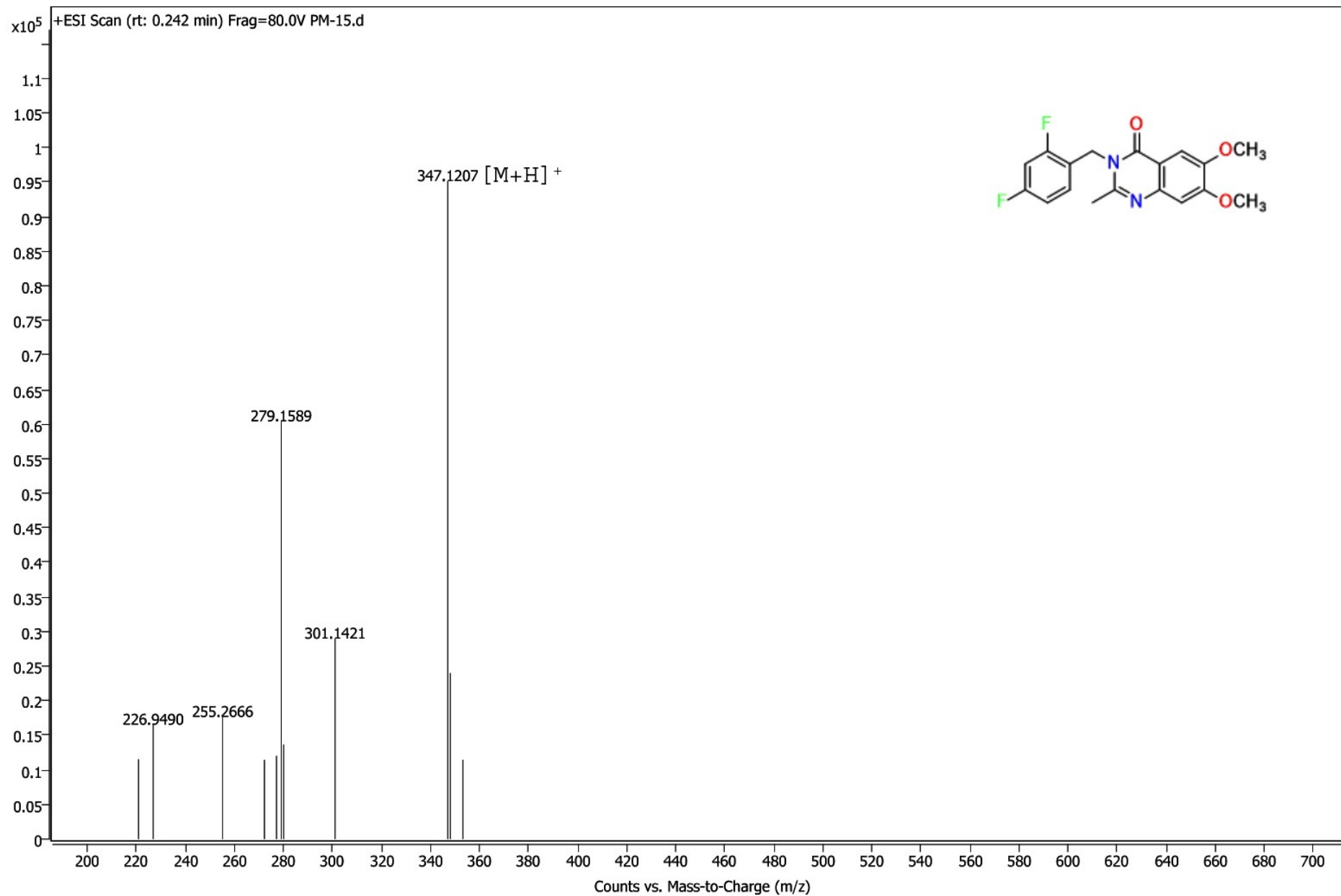
$^1\text{H}$  NMR of **4e**



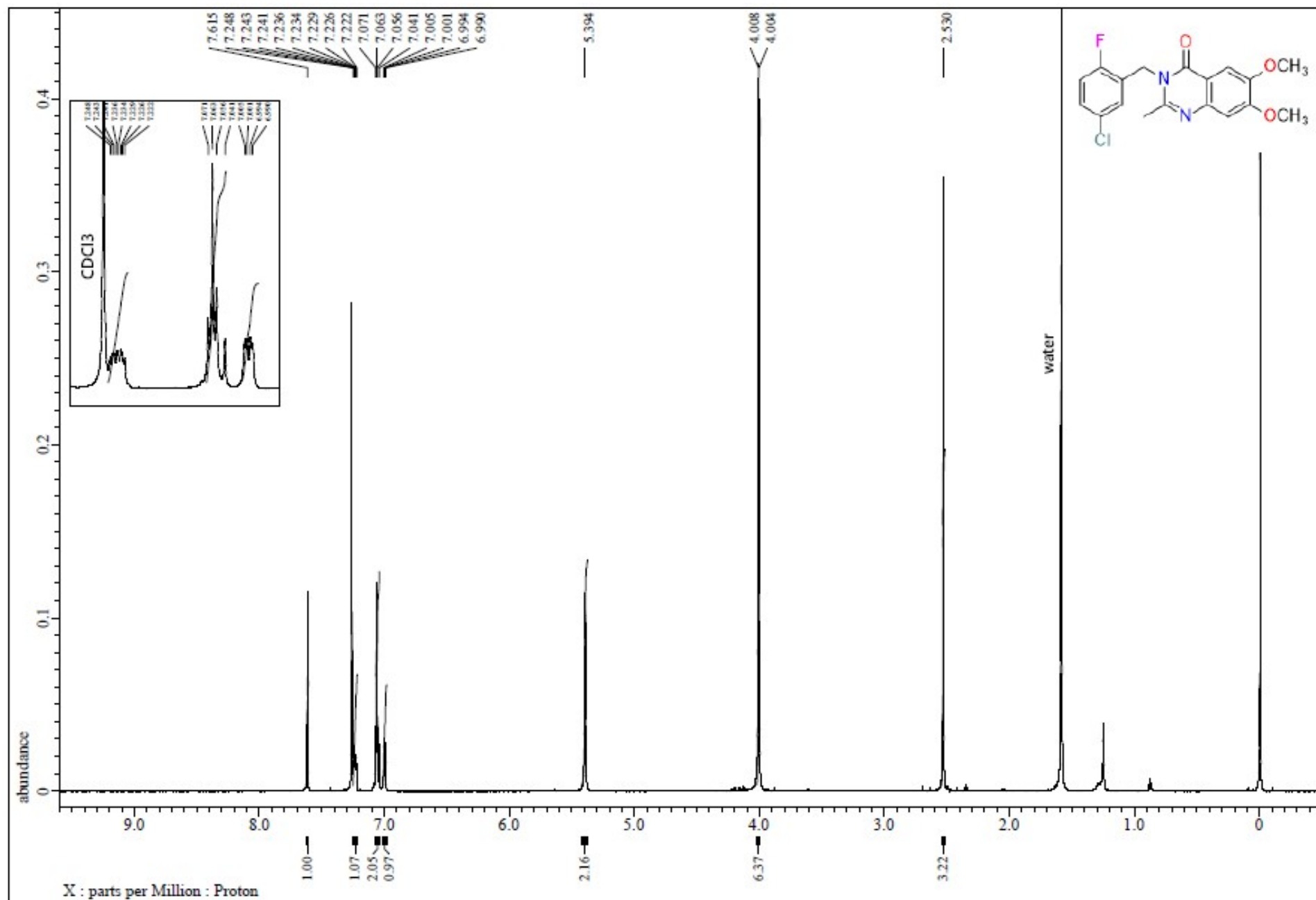
<sup>13</sup>C NMR of 4e



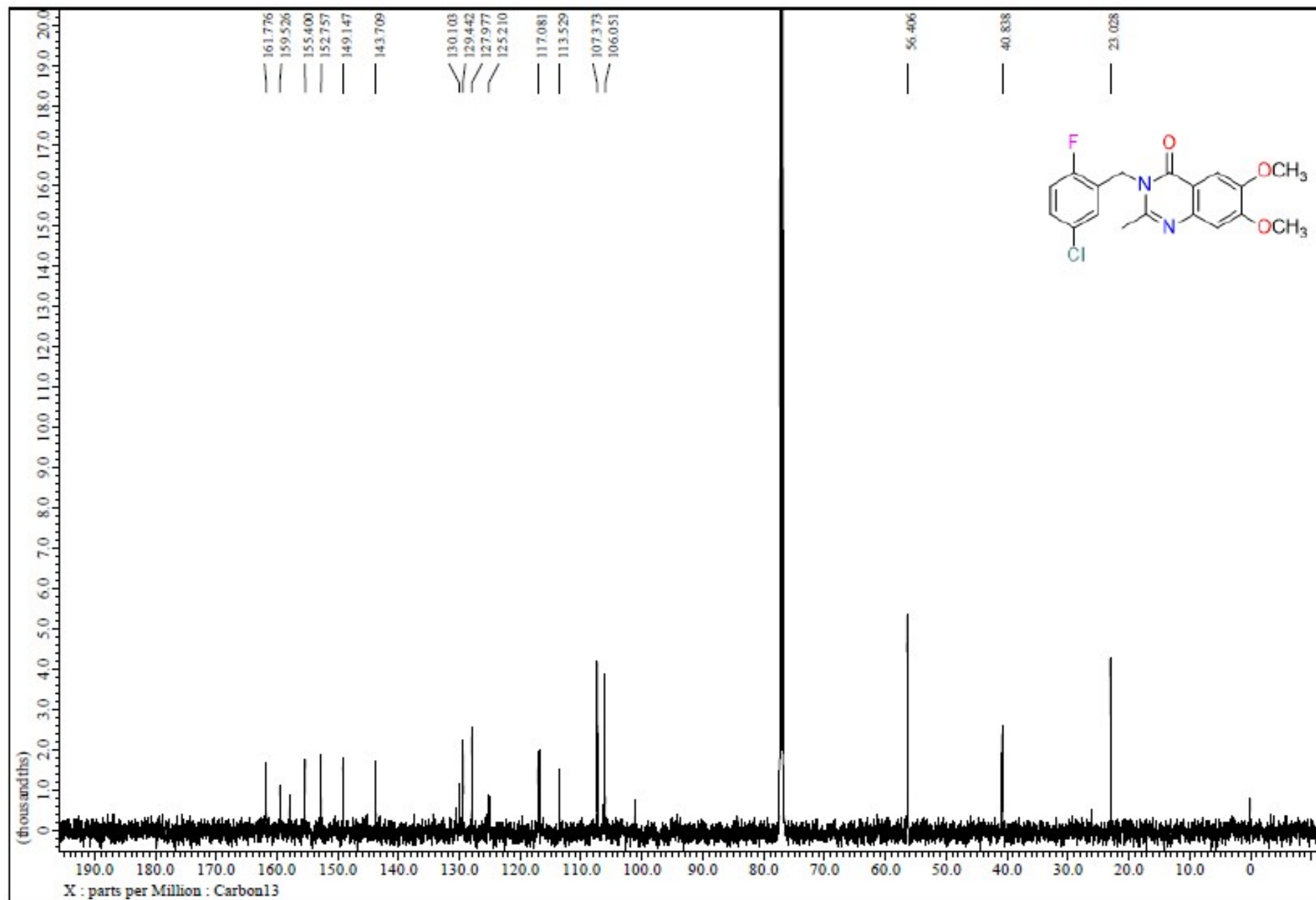
# HRMS of 4e



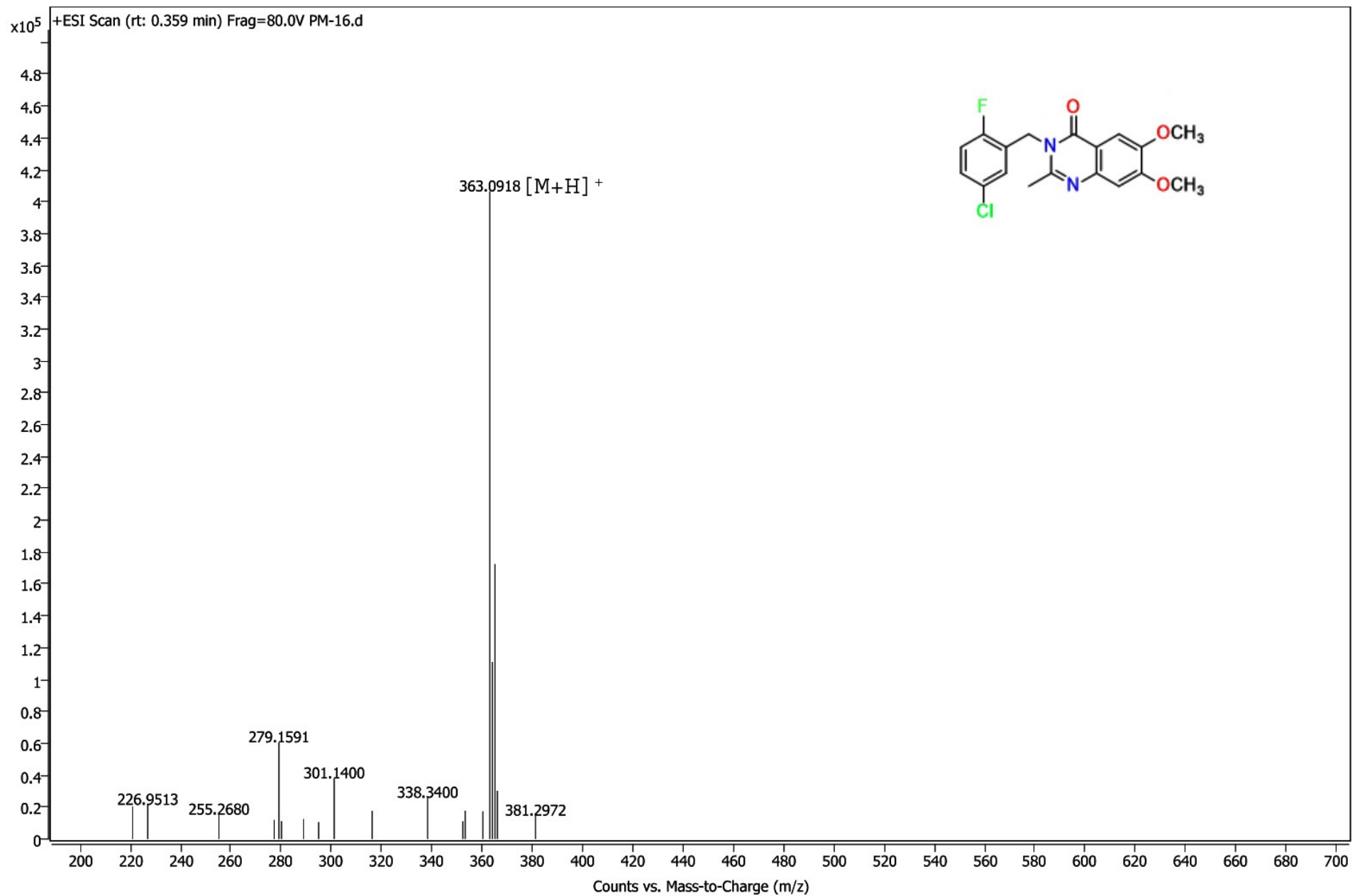
<sup>1</sup>H NMR of 4f



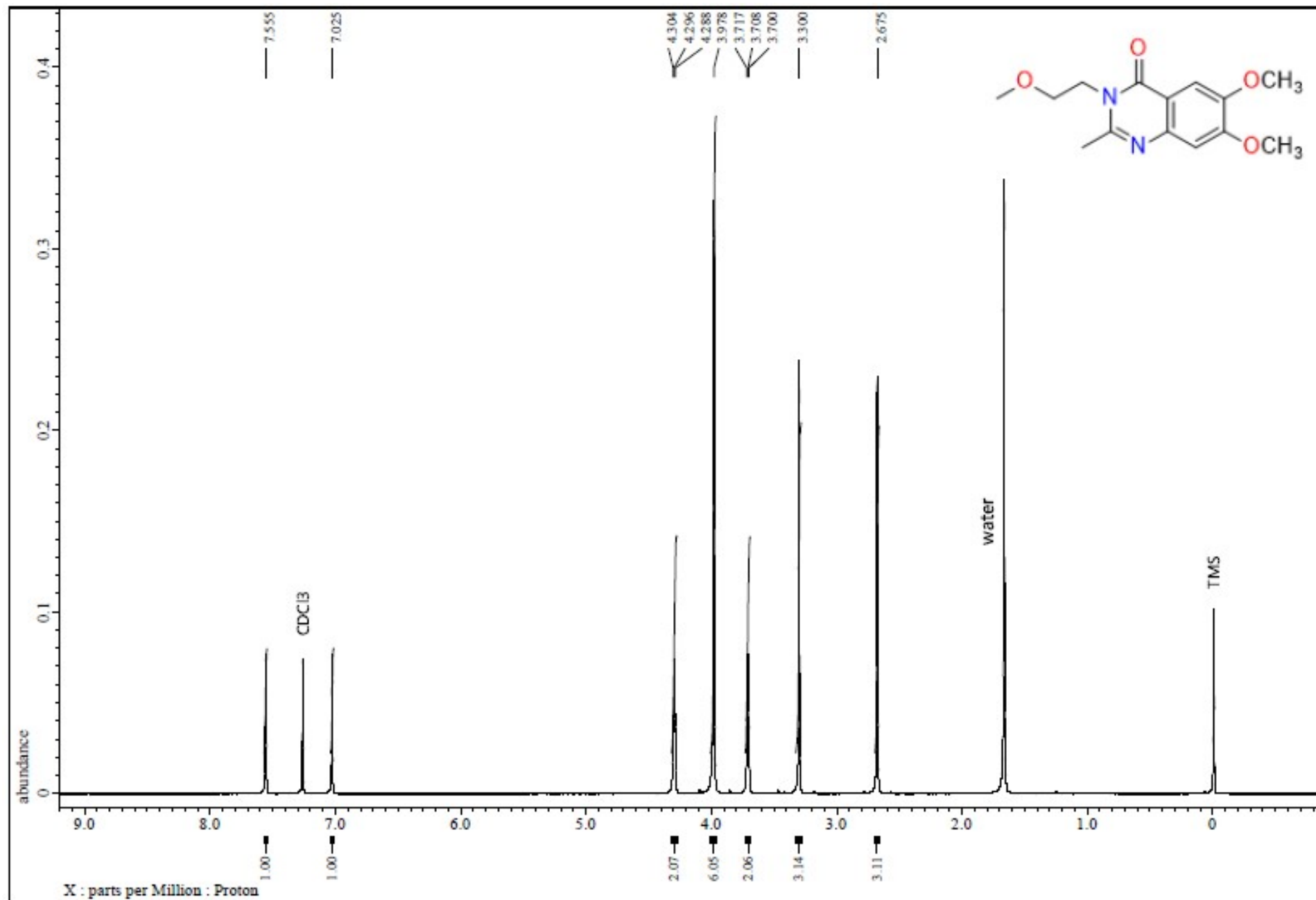
<sup>13</sup>C NMR of **4f**



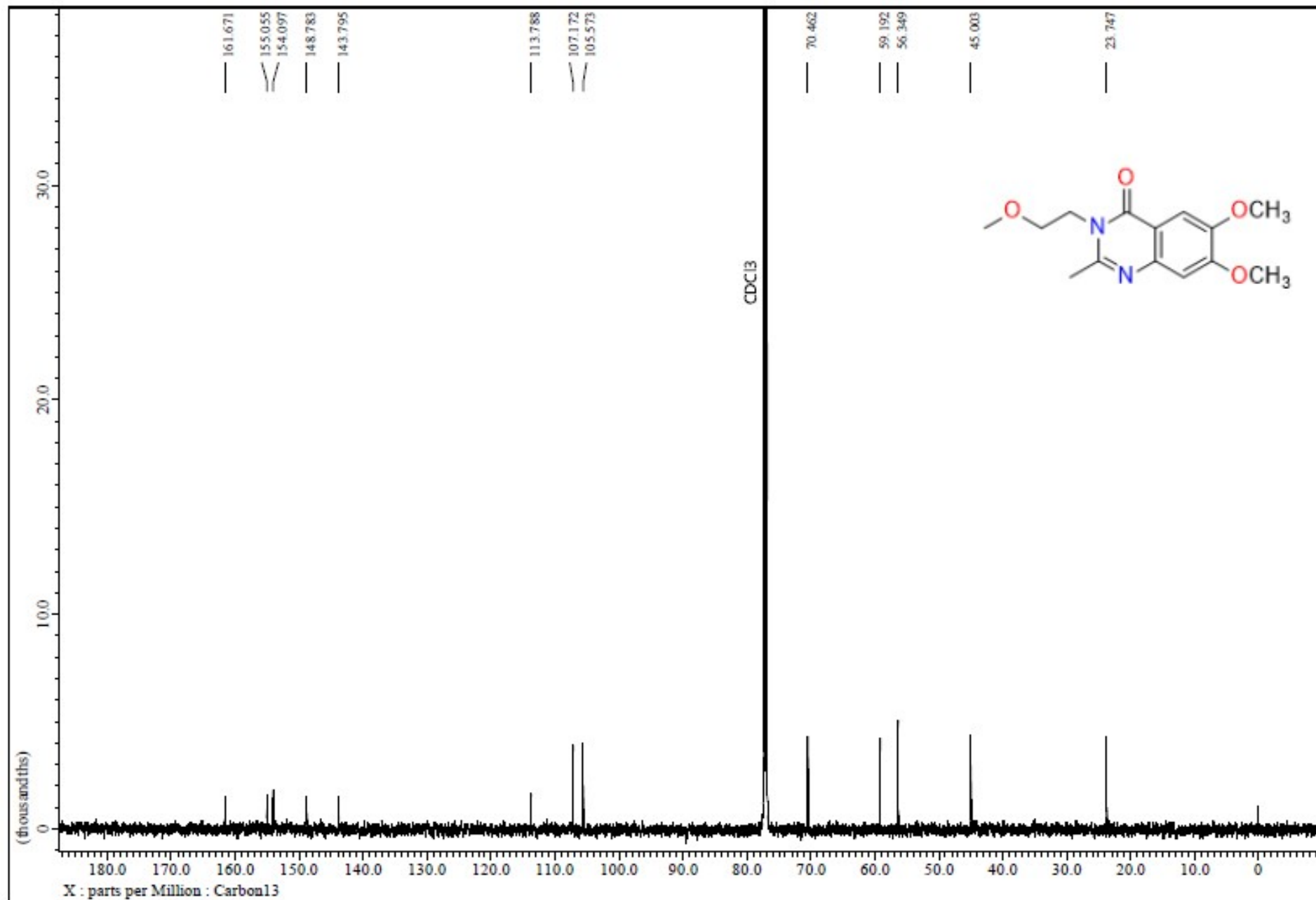
# HRMS of 4f



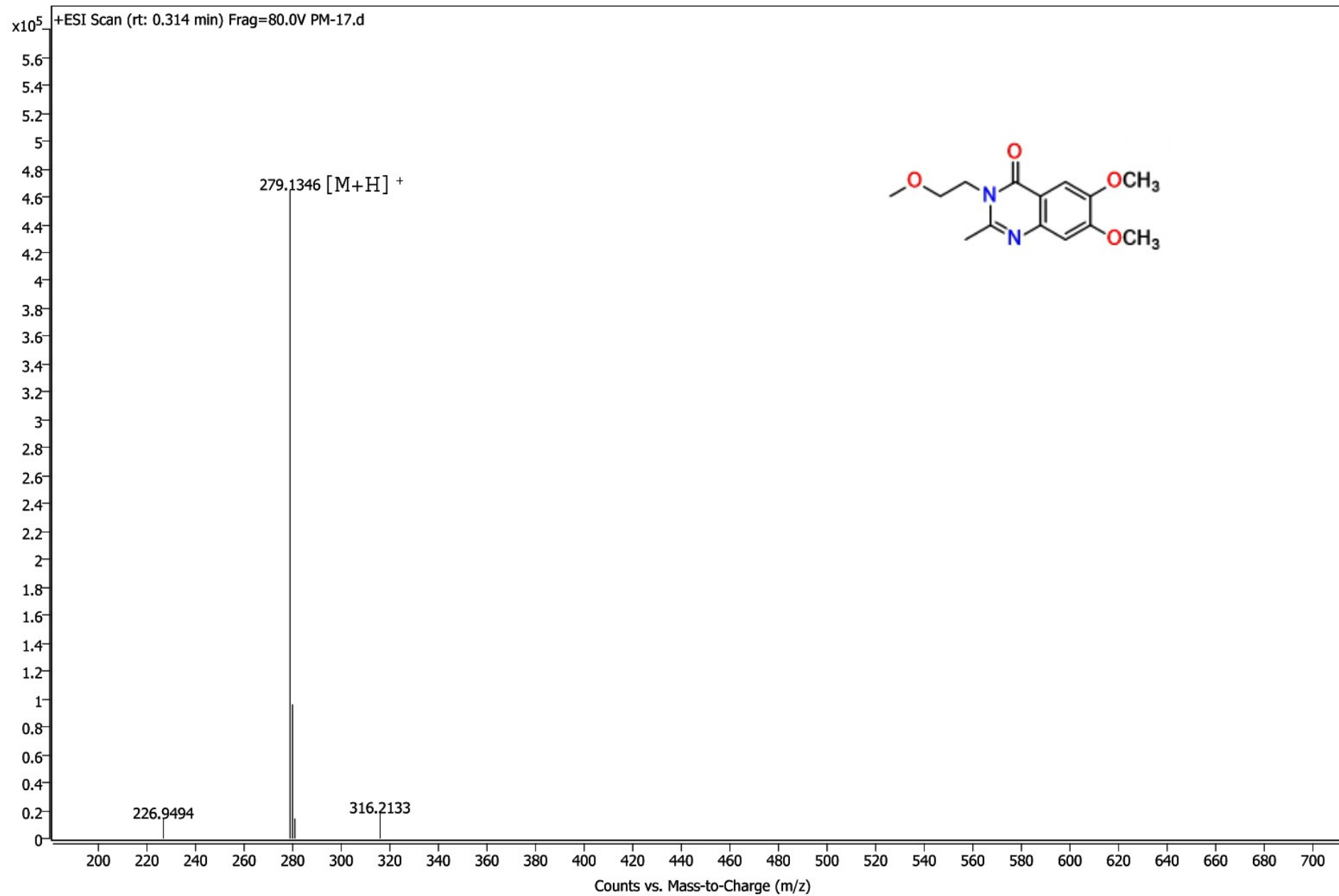
$^1\text{H}$  NMR of **4g**



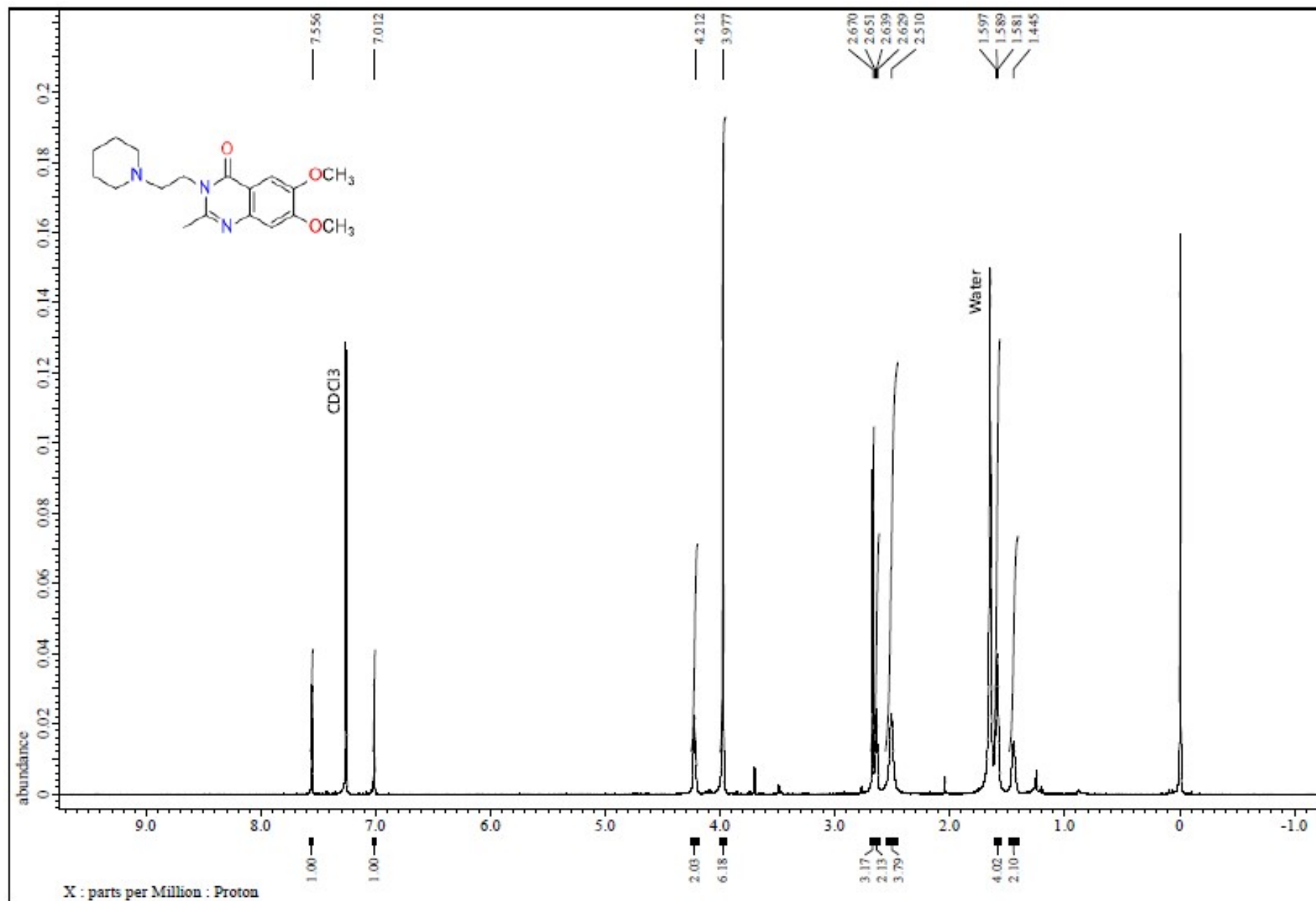
<sup>13</sup>C NMR of **4g**



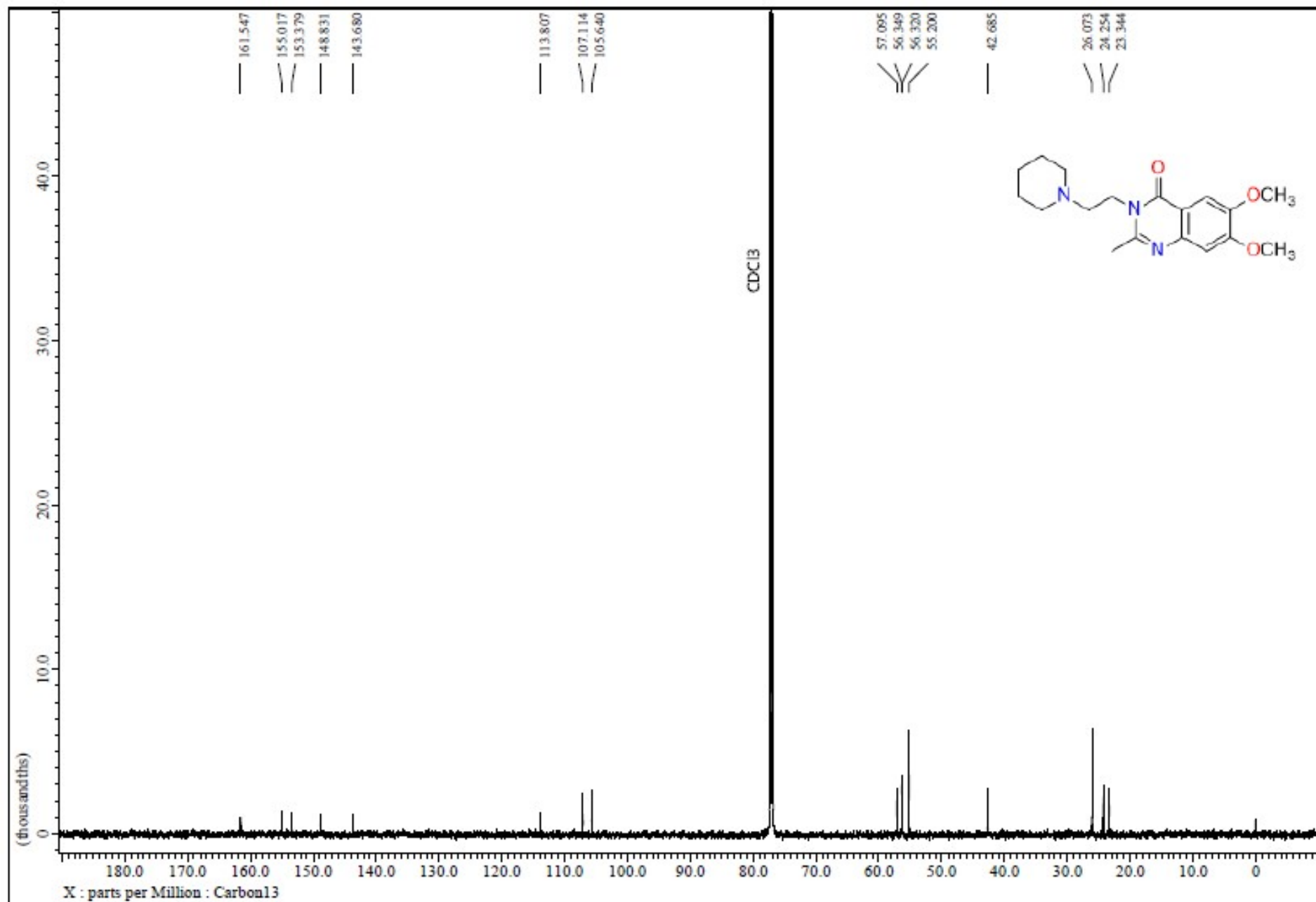
# HRMS of 4g



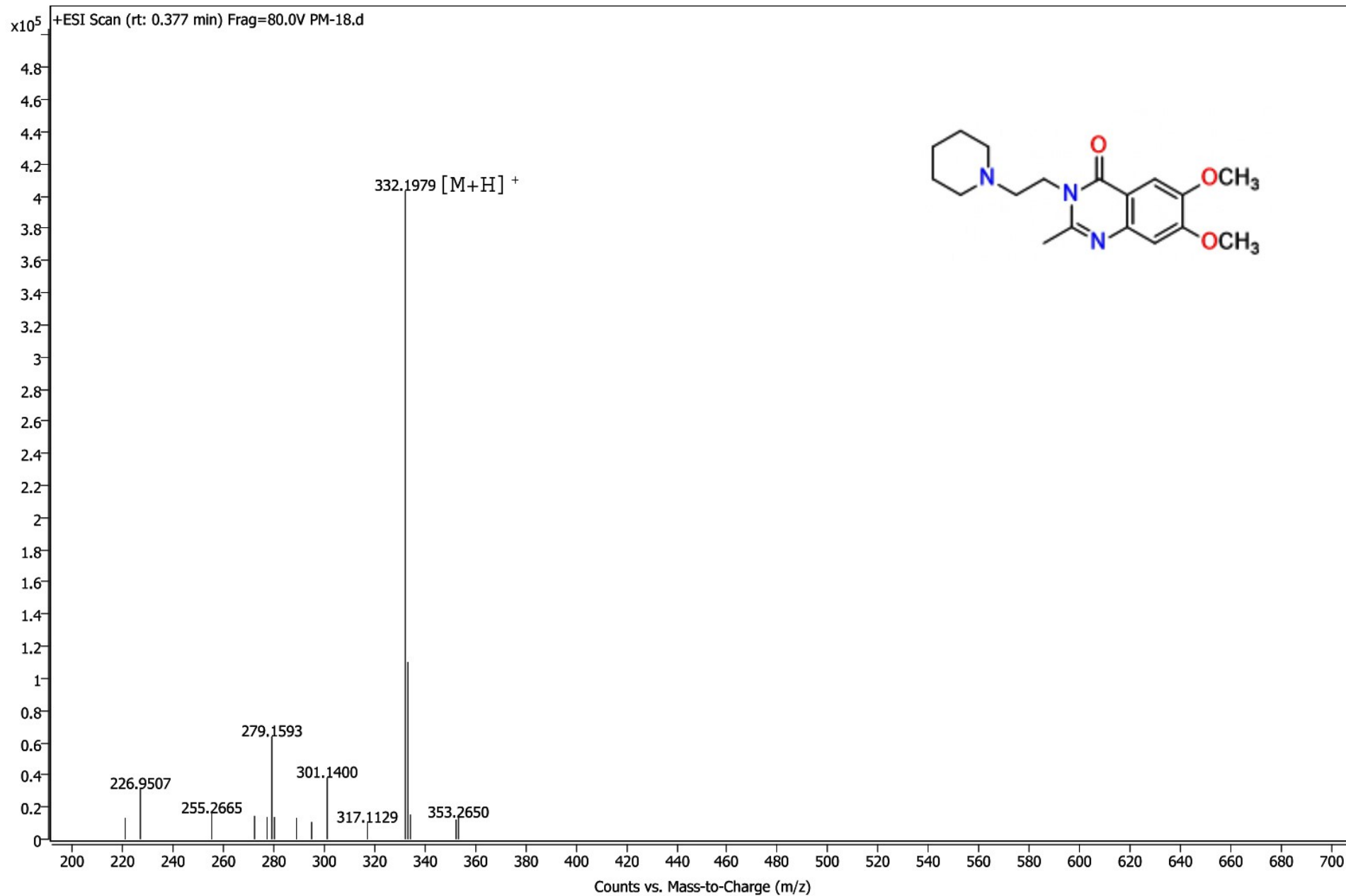
<sup>1</sup>H NMR of 4h



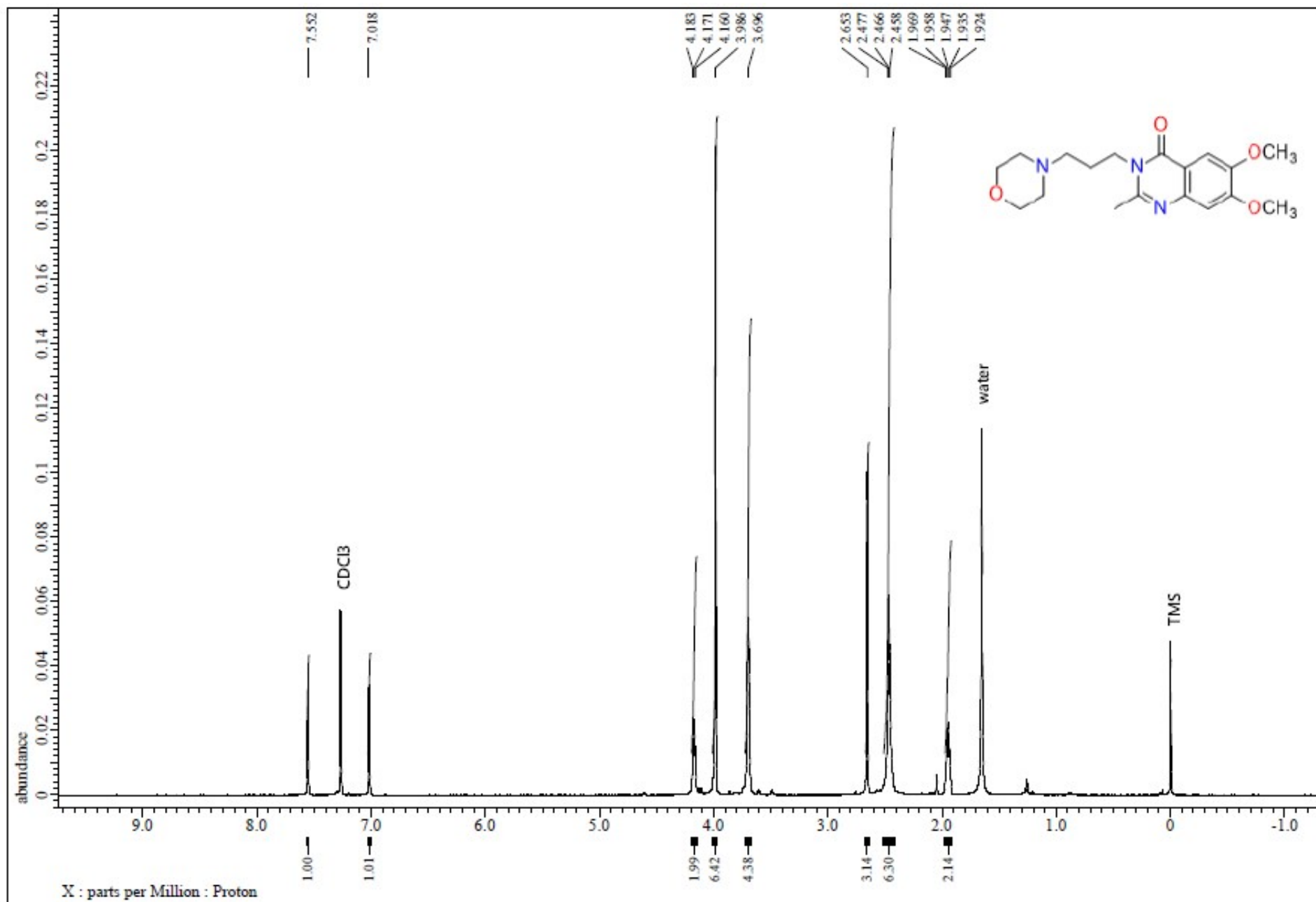
<sup>13</sup>C NMR of 4h



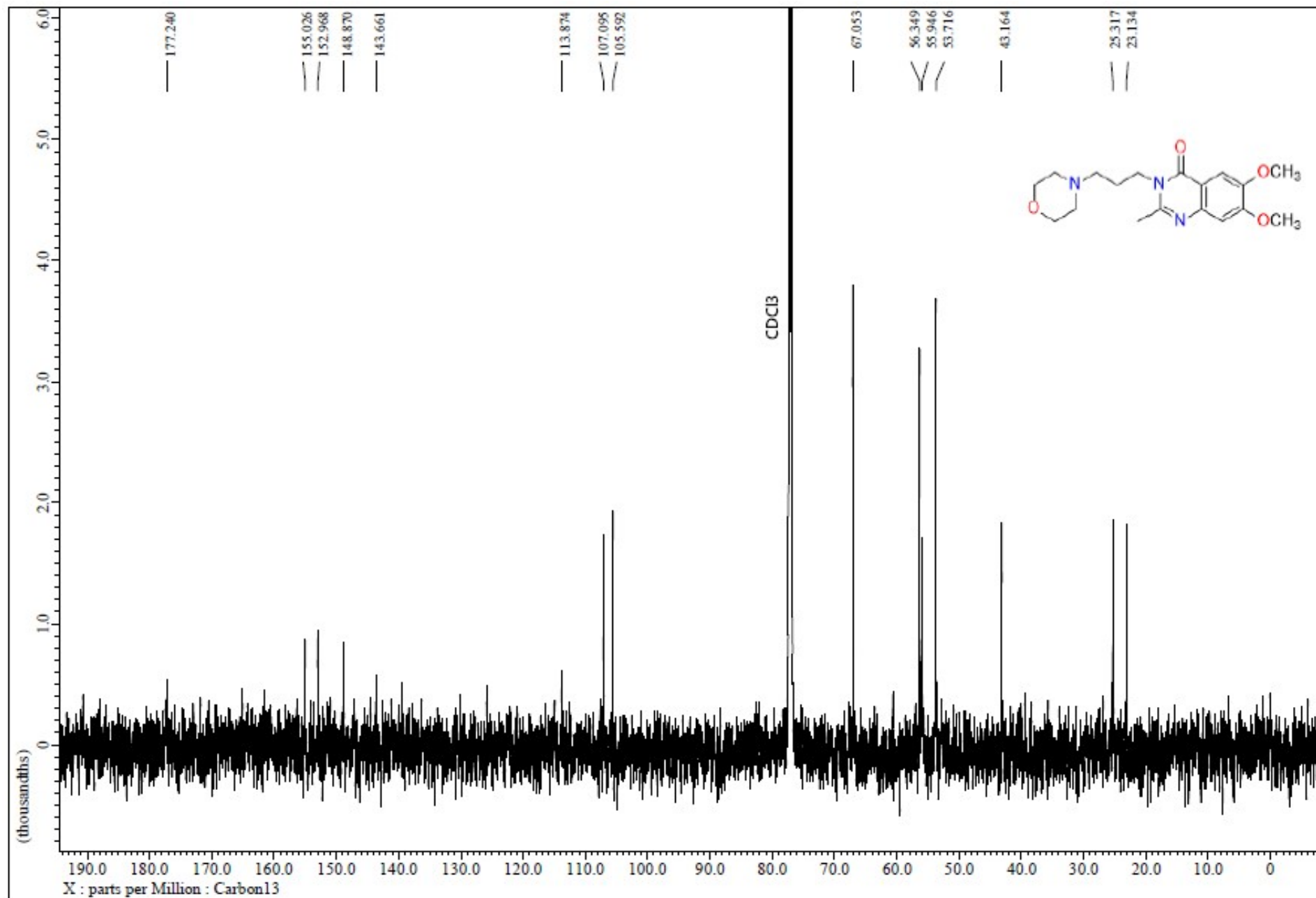
# HRMS of 4h



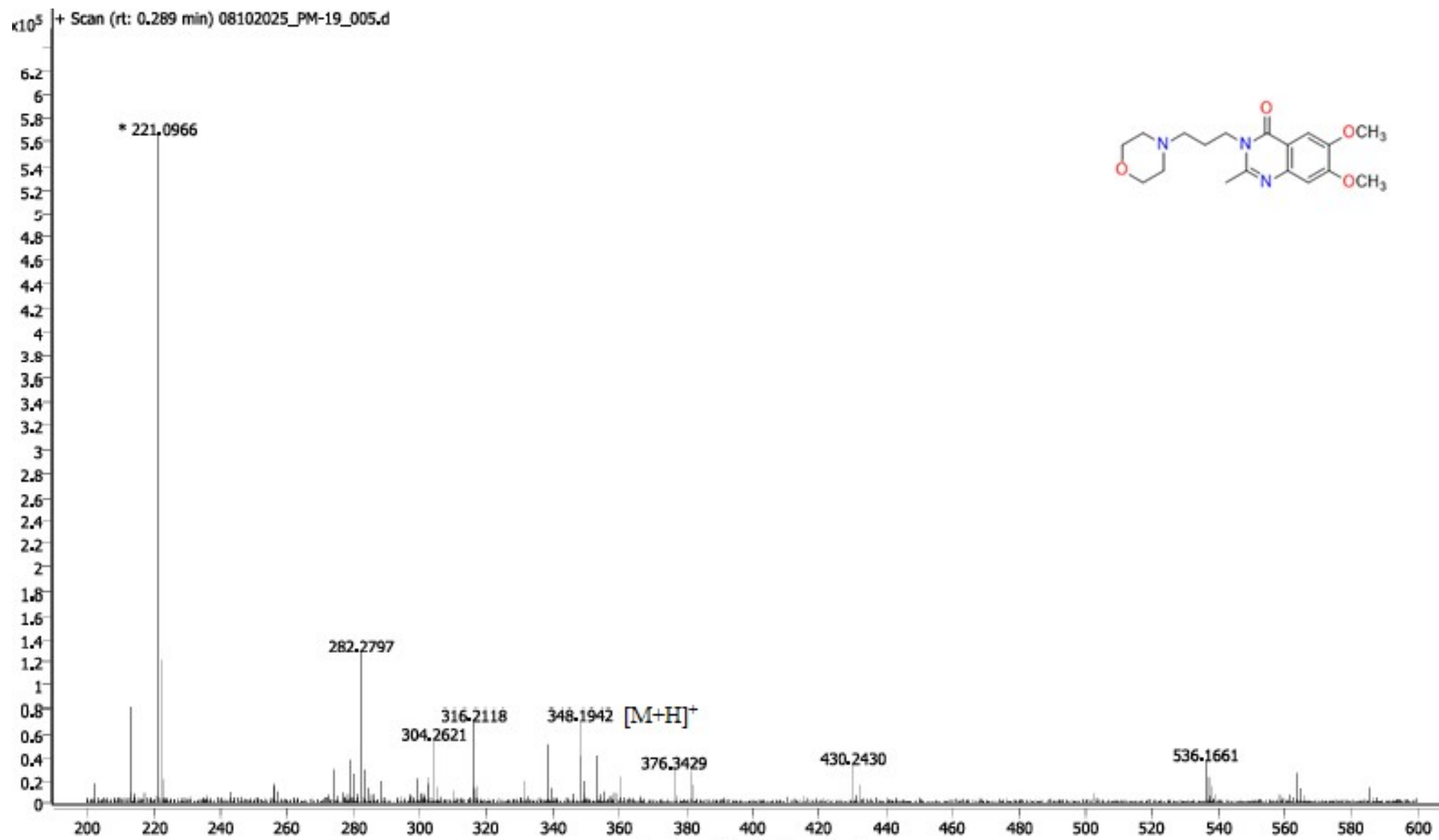
<sup>1</sup>H NMR of 4i



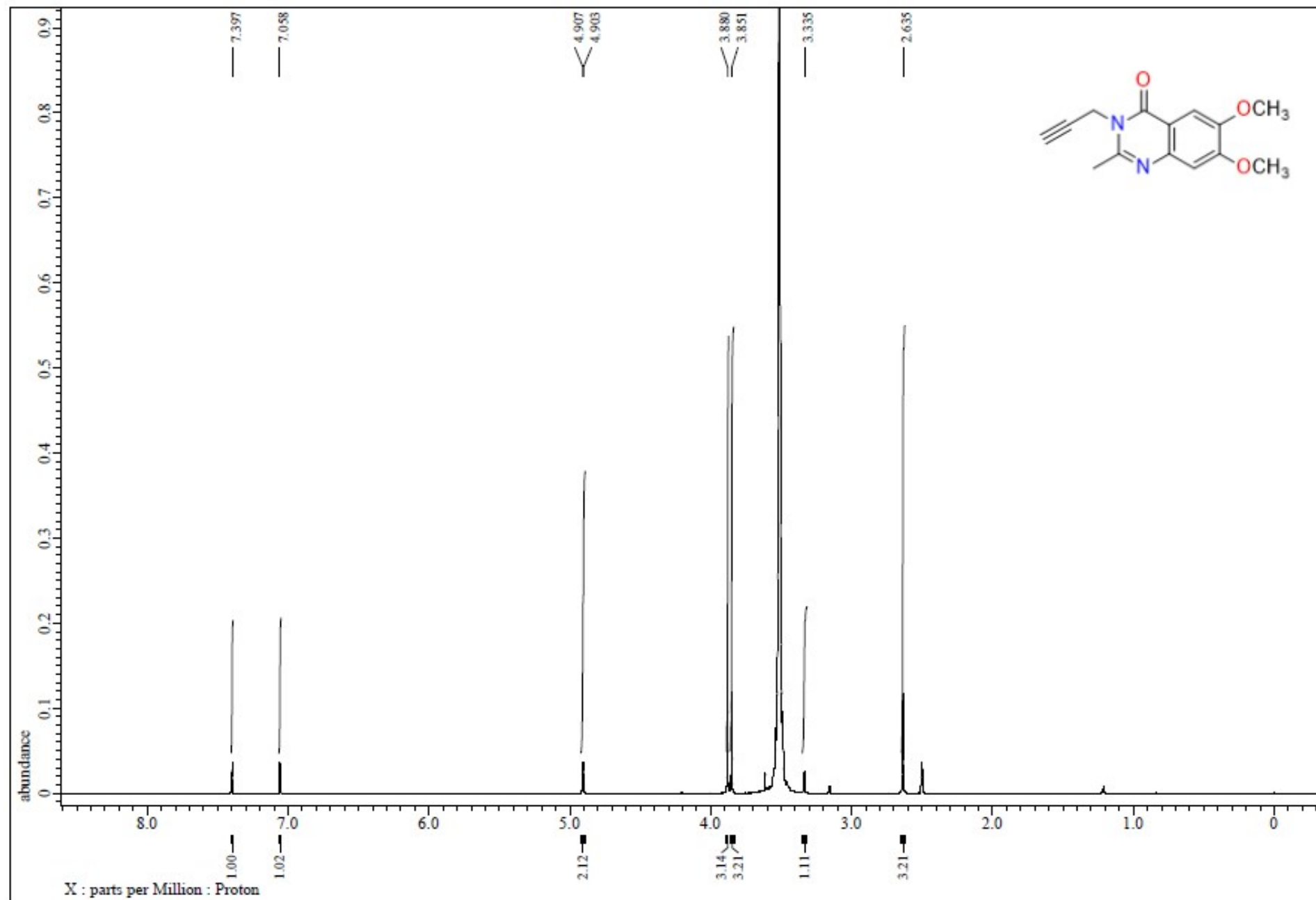
<sup>13</sup>C NMR of **4i**



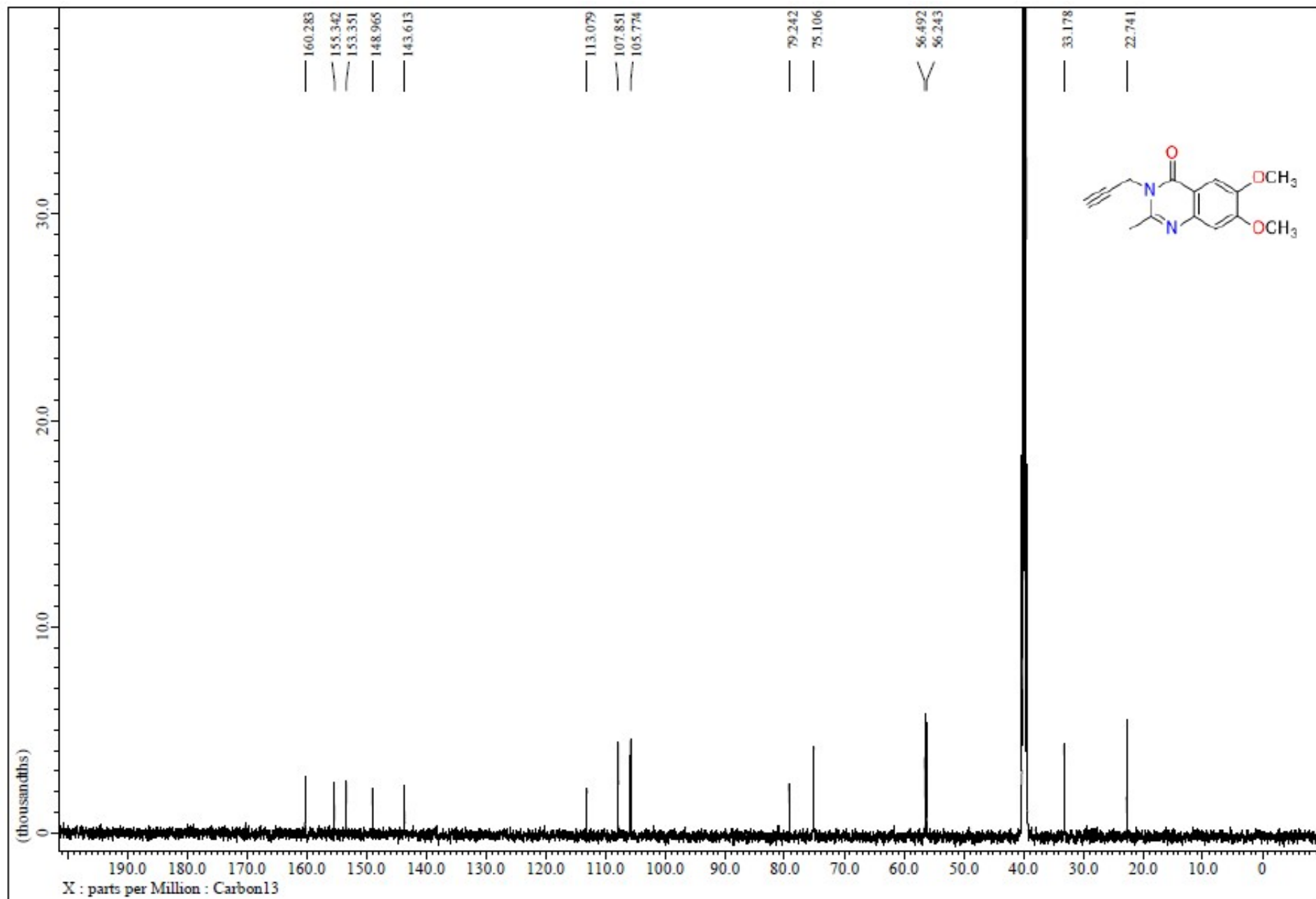
# HRMS of 4i



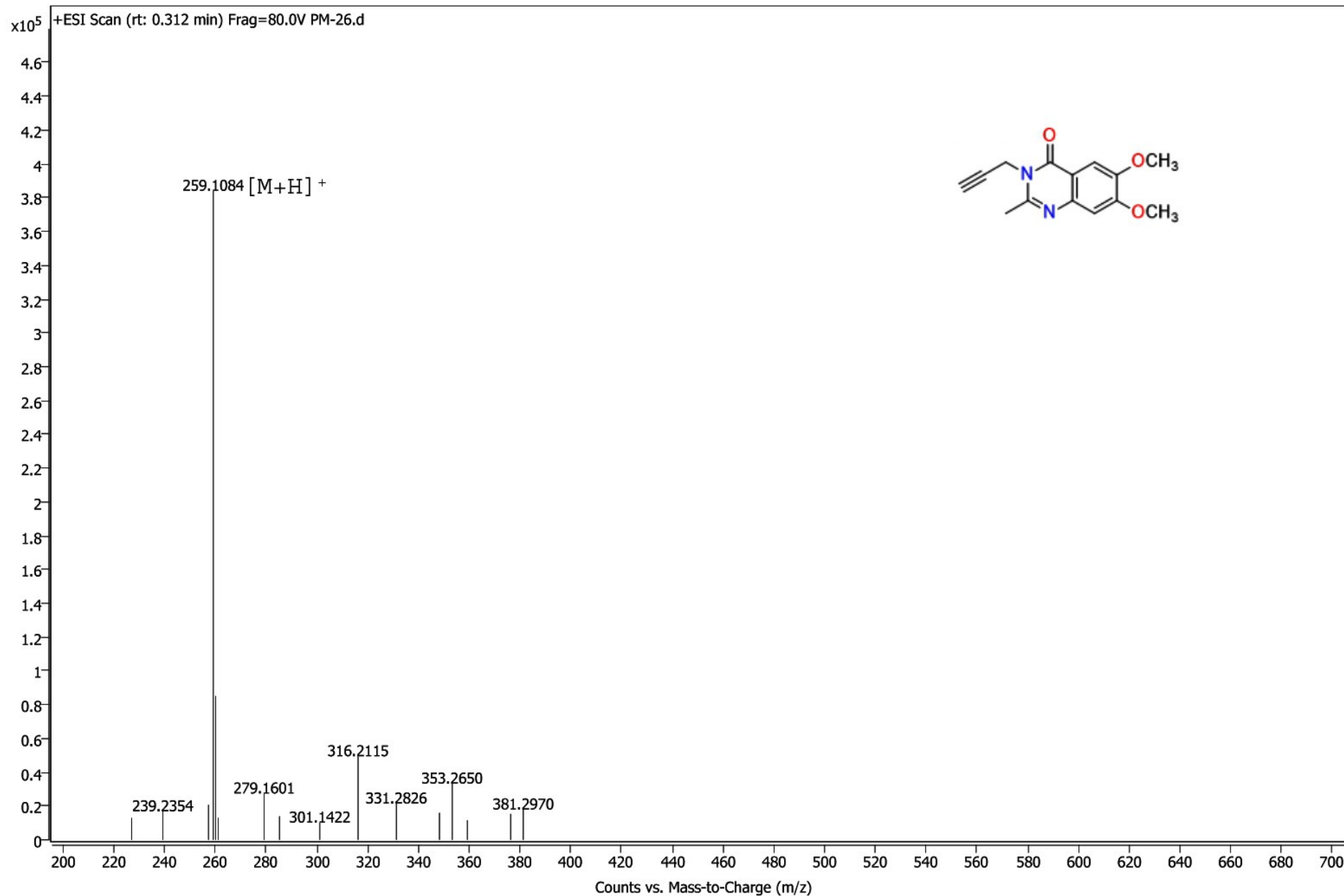
<sup>1</sup>H NMR of 4j



<sup>13</sup>C NMR of 4j



# HRMS of 4j

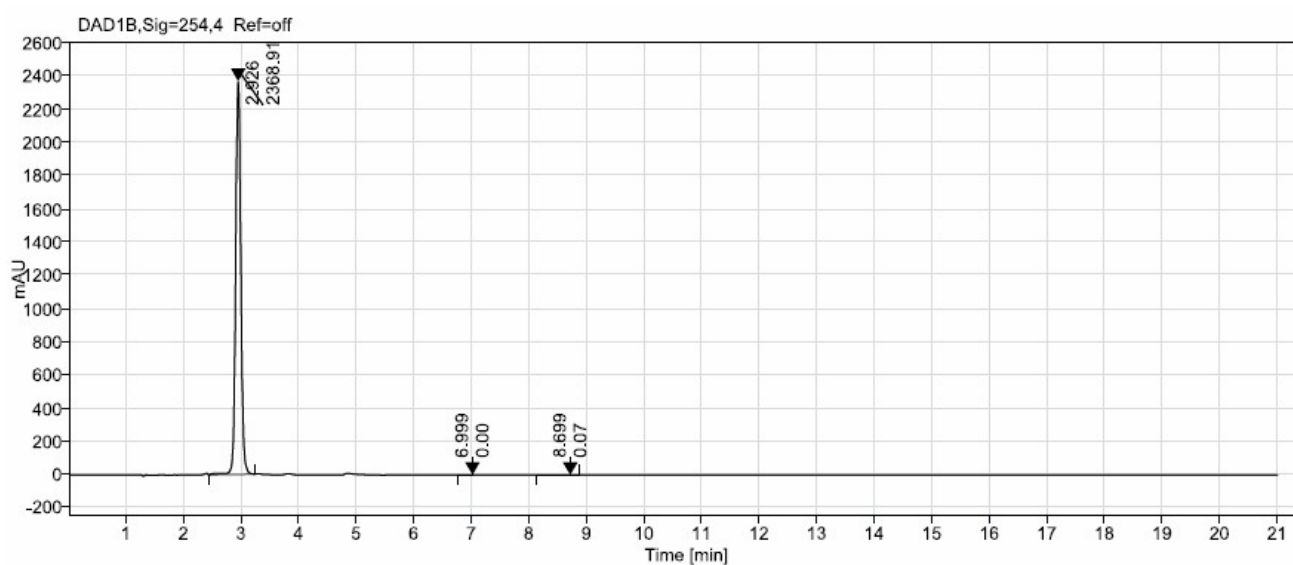


## HPLC method and % purity of all synthesized final compounds (4a-4j)

### HPLC method

An Agilent 1260 Infinity II system was used for HPLC analysis. The UV-Vis detector DAD 1260WAR, autosampler G7129A, and a Hypersil C-18 column (4.6 × 250 mm) were used in the system. The study was performed at 25–28°C using a mobile phase consisting of water (A) and acetonitrile (B) with a flow rate of 1 mL/min. The gradient program started with 40% water and 60% acetonitrile at 0.00 min followed by 30% water and 70% acetonitrile for 3.00 min, 10% water and 90% acetonitrile at 7.00 min, 0% water and 100% acetonitrile for 10.00 min. The total run time was 20 minutes. The maximum pressure limit was set to 400 bar throughout the run.

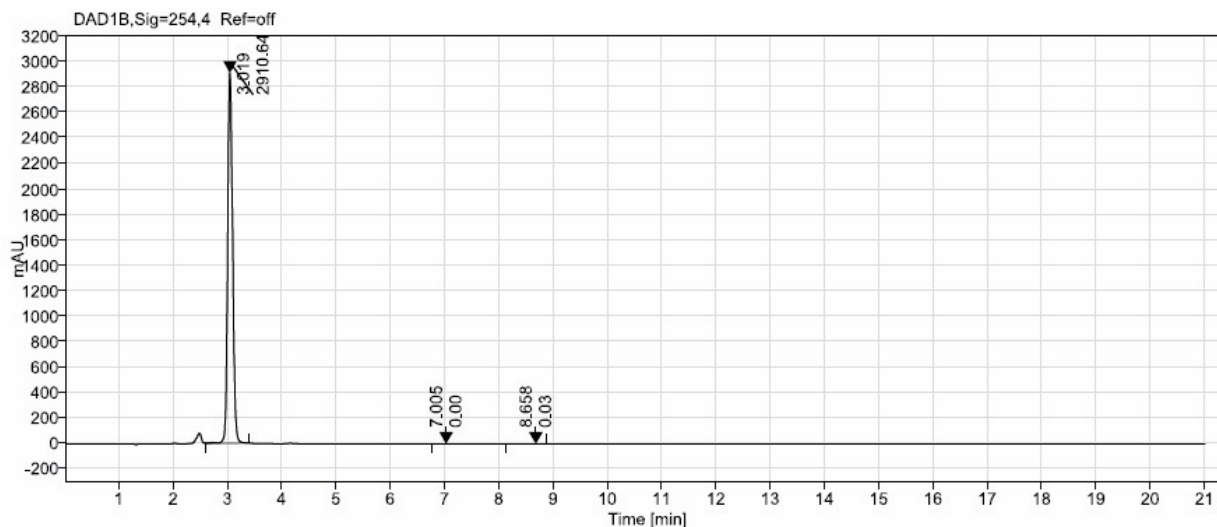
### HPLC of 4a



Signal: DAD1B, Sig=254,4 Ref=off

Name	RT [min]	Area	Area %	Height	Height %
	2.926	14698.418	100.00	2368.907	100.00
	6.999	0.156	0.00	0.000	0.00
	8.699	0.343	0.00	0.074	0.00

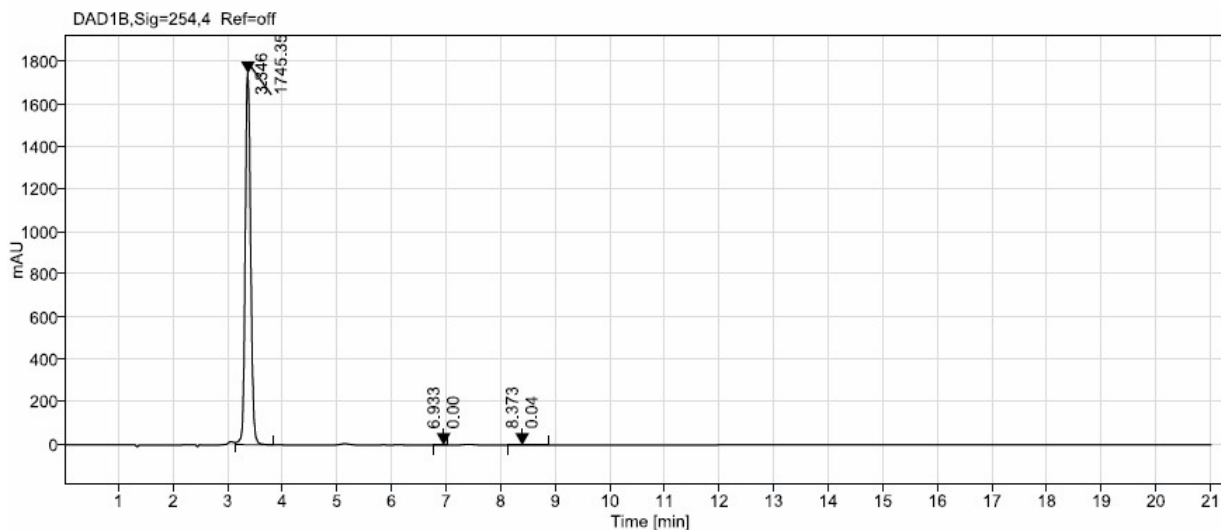
## HPLC of 4b



Signal: DAD1B,Sig=254,4 Ref=off

Name	RT [min]	Area	Area %	Height	Height %
	3.019	18444.005	99.99	2910.635	100.00
	7.005	0.281	0.00	0.002	0.00
	8.658	1.060	0.01	0.026	0.00

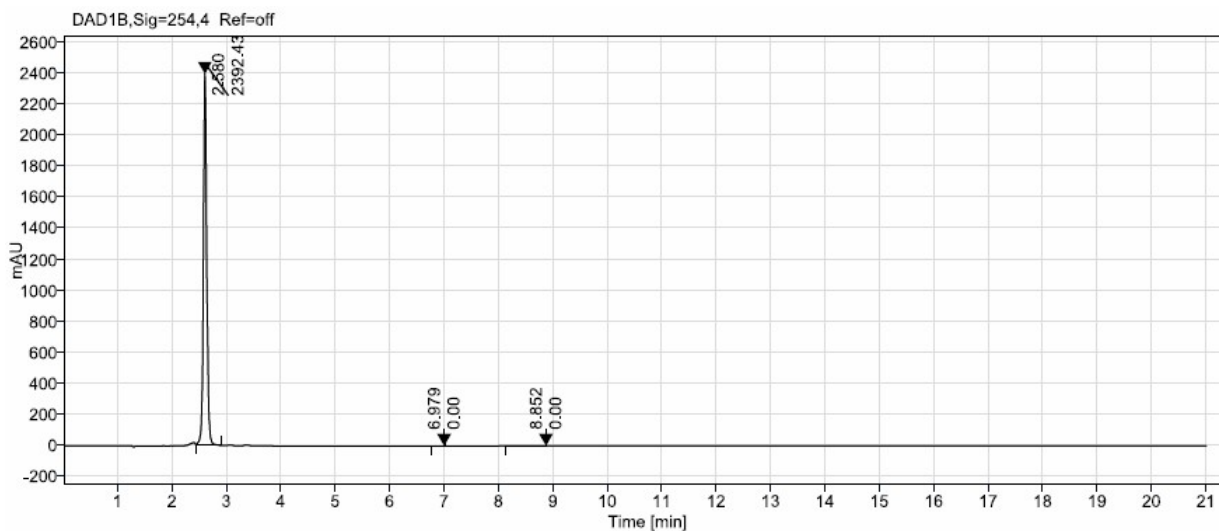
## HPLC of 4c



Signal: DAD1B,Sig=254,4 Ref=off

Name	RT [min]	Area	Area %	Height	Height %
	3.346	11962.702	99.99	1745.351	100.00
	6.933	0.025	0.00	0.004	0.00
	8.373	1.006	0.01	0.045	0.00

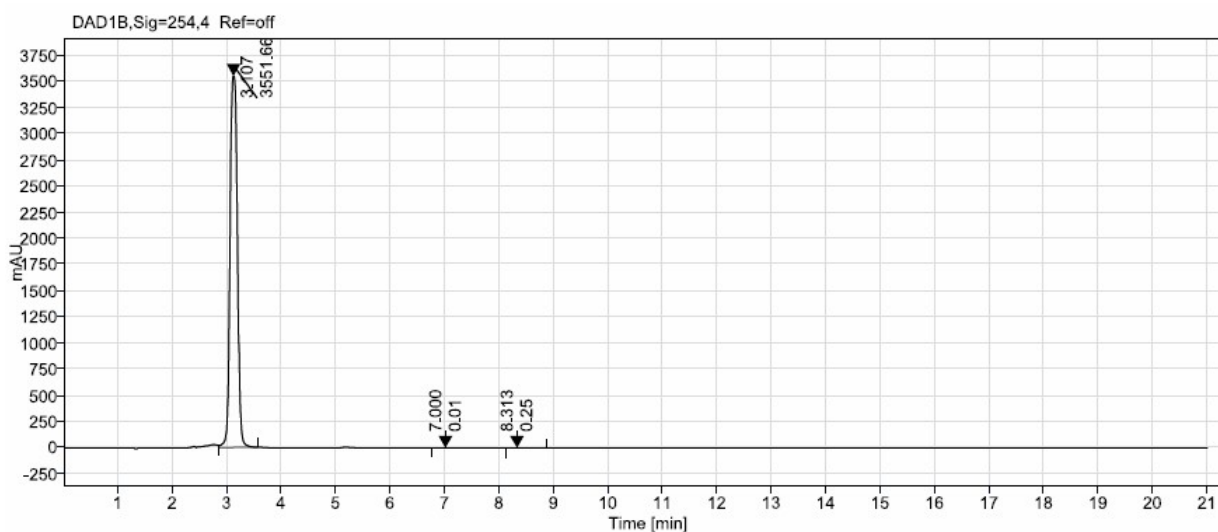
## HPLC of 4d



Signal: DAD1B,Sig=254,4 Ref=off

Name	RT [min]	Area	Area %	Height	Height %
	2.580	10408.209	99.99	2392.427	100.00
	6.979	0.019	0.00	0.003	0.00
	8.852	0.528	0.01	0.000	0.00

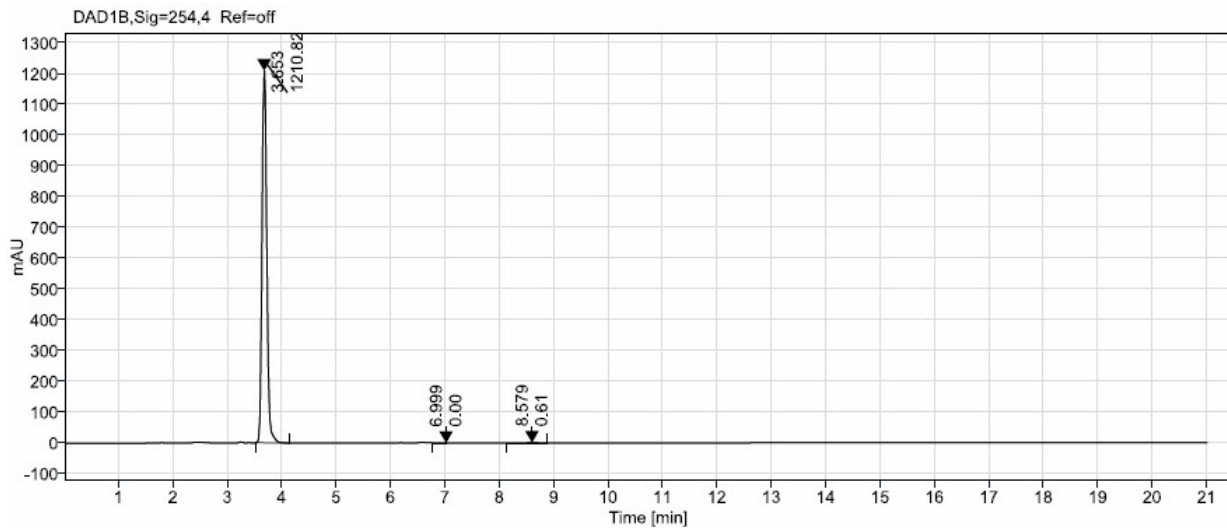
## HPLC of 4e



Signal: DAD1B,Sig=254,4 Ref=off

Name	RT [min]	Area	Area %	Height	Height %
	3.107	33000.670	99.98	3551.657	99.99
	7.000	1.468	0.00	0.008	0.00
	8.313	4.443	0.01	0.251	0.01

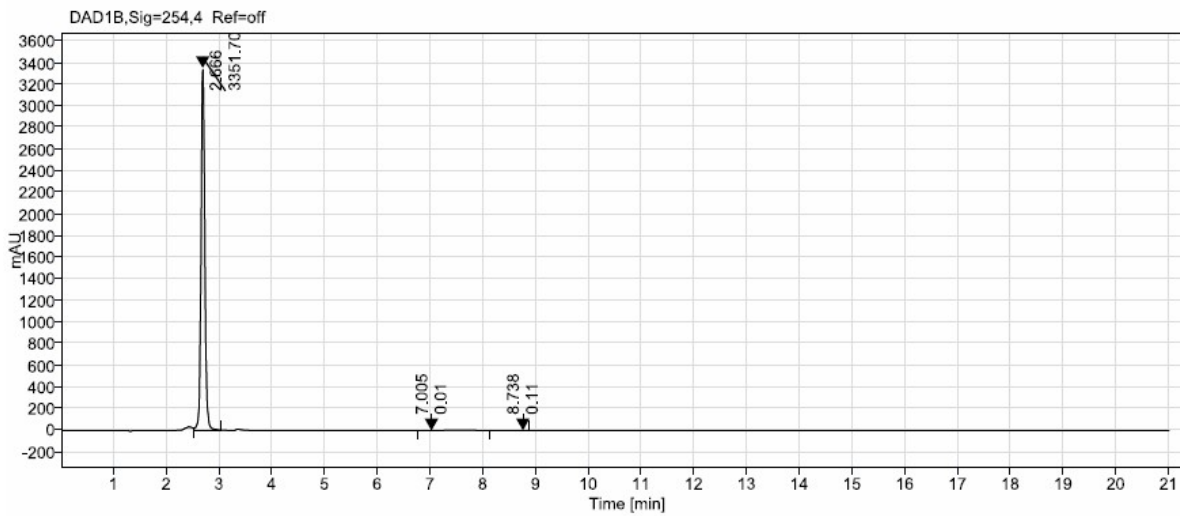
## HPLC of 4f



Signal: DAD1B,Sig=254,4 Ref=off

Name	RT [min]	Area	Area %	Height	Height %
	3.653	7314,850	99,91	1210,824	99,95
	6.999	0.539	0.01	0.000	0.00
	8.579	5.938	0.08	0.606	0.05

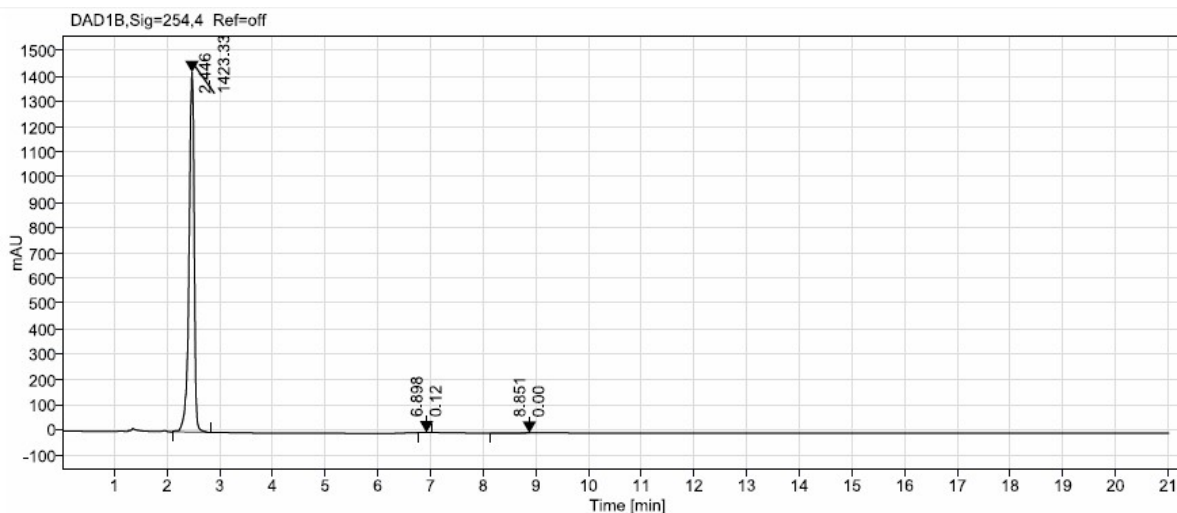
## HPLC of 4g



Signal: DAD1B,Sig=254,4 Ref=off

Name	RT [min]	Area	Area %	Height	Height %
	2.666	17057.110	99.96	3351.697	100.00
	7.005	0.439	0.00	0.012	0.00
	8.738	6.617	0.04	0.109	0.00

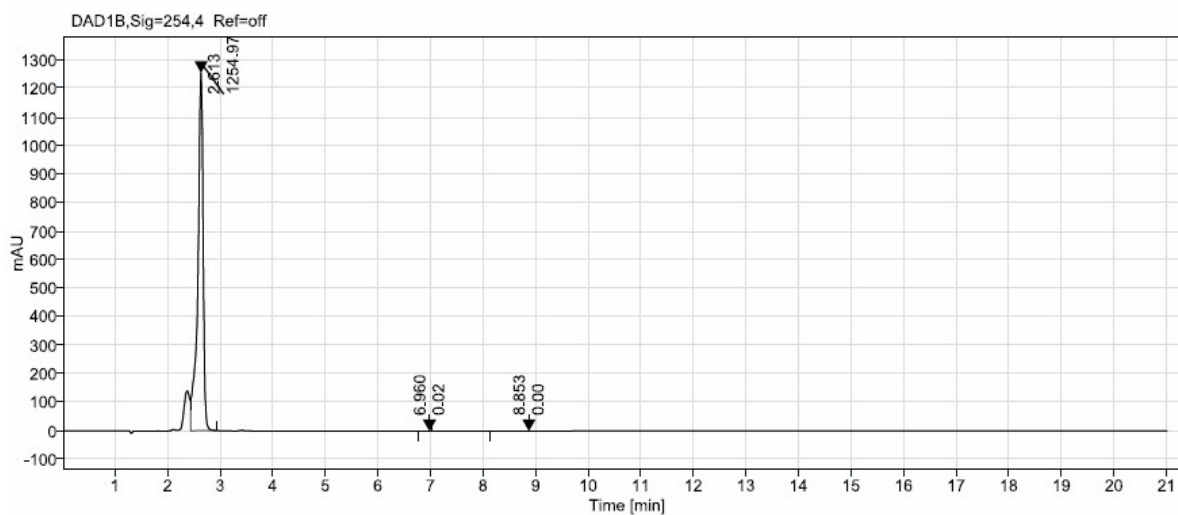
## HPLC of 4i



Signal: DAD1B,Sig=254,4 Ref=off

Name	RT [min]	Area	Area %	Height	Height %
	2.446	9603.727	99.98	1423.329	99.99
	6.898	1.278	0.01	0.118	0.01
	8.851	1.057	0.01	0.000	0.00

## HPLC of 4j



Signal: DAD1B,Sig=254,4 Ref=off

Name	RT [min]	Area	Area %	Height	Height %
	2.613	8722.115	99.99	1254.972	100.00
	6.960	0.288	0.00	0.021	0.00
	8.853	0.349	0.00	0.000	0.00